INTERFERENCE ANALYSIS OF MASSIVE MIMO DOWNLINK WITH MRT PRECODING AND APPLICATIONS IN PERFORMANCE ANALYSIS

by

Chi Feng

A thesis submitted in partial fulfillment of the requirements for the degree of

Master of Science
in
Communications

Department of Electrical and Computer Engineering
University of Alberta

Abstract

Recently, massive MIMO (multiple-input-multiple-output) systems, where the base station (BS) is equipped with hundreds of small, low-cost, and low-power antennas, have been proposed as one of the promising technologies for the next generation cellular systems.

The thesis works on the performance analysis of single-cell multi-user massive MIMO downlink. Perfect channel state information (CSI) is assumed at the BS and maximum ratio transmission (MRT) precoding scheme is adopted. We first investigate the distribution of the interference power and derive its probability density function (pdf) by central limit theory. After that, analytical results on the outage probability and the sum-rate are derived. Different to existing work using the law of large numbers to derive the asymptotic deterministic signal-to-interference-plus-noise-ratio (SINR), the randomness of the interference in the SINR is kept intact in our work, which allows the derivation of the outage probability. We further extend to networks with per-antenna power constraint. A modified MRT precoding scheme is proposed and the performance of the modified scheme is analyzed. Our work show that the modified MRT precoding can achieve lower outage probability and higher sum-rate than MRT precoding, even with more strict power constraint.

Acknowledgments

I would like to thank all the people who contributed in some way to the work described in this thesis. First and foremost, I am deeply indebted to my academic advisors, Dr. Yindi Jing. Her guidance and supervision help me to learn how to be a good researcher and pursue an academic career.

I also would like to acknowledge friends and family who supported me during my time here. First and foremost I would like to thank Mom, Dad and other family members for their constant love and support. Additionally, I am lucky to have met lots of good friends here and have a happy life. Thanks for their friendship and unyielding support.

Table of Contents

List of Figures

List of Abbreviations

Acronyms	Definition
1G	First Generation Cellular Systems
2G	Second Generation Cellular Systems
3G	Third Generation Cellular Systems
4G	Fourth Generation Cellular Systems
5G	Fifth Generation Cellular Systems
BS	Base Station
CDMA	Code Division Multiple Access
CE	Constant Envelope
CSI	Channel State Information
GSM	Global System for Mobile Communication
LTE	Long Term Evolution
MF	Matched Filter
MGF	Moment Generating Function
MIMO	Multiple-Input Multiple-Output
MMSE	Minimum-Mean-Square-Error
mmWave	Millimeter Wave
MRT	Maximum-Ratio Transmission
PA	Power Amplifier
pdf	Probability Density Function
SINR	Signal-to-Interference-plus-Noise-Ratio
TDD	Time Division Duplex
TDMA	Time Division Multiple Access

WF	Wiener Filter
ZF	Zero-Forcing

Chapter 1

Introduction

Wireless communications is undoubtedly one of the most important technologies in the world for the past decades. Its great success is not only attributed to the outstanding achievements from a scientific point of view, but also to the great impact on the whole human society. People's lifestyle has been changed hugely by wireless communications.

To the history of wireless communications, it can date back to 150 years ago. In 1865, Maxwell proposed the prediction of the existence of the electromagnetic waves with the publication of *"A Dynamical Theory of the Electromagnetic Field"* [1]. In 1888, Hertz proved Maxwell's electromagnetic theory via experiments. Then the basic understandings of the electromagnetic wave transmissions had been established. In 1898, Marconi made successful demonstrations of wireless transmission in public. He is widely known as the inventor of wireless communications and received the Nobel Prize for his great contributions of wireless telegraphy in 1909. Since then, wireless communications drew widespread interests over the world. In this chapter, a brief introduction of wireless systems is given.

1.1 Fading in Wireless Channel

In wireless communications, the fading effect in wireless channel is always a great challenge. Fading can be categorized as small-scale fading and large-scale fading.

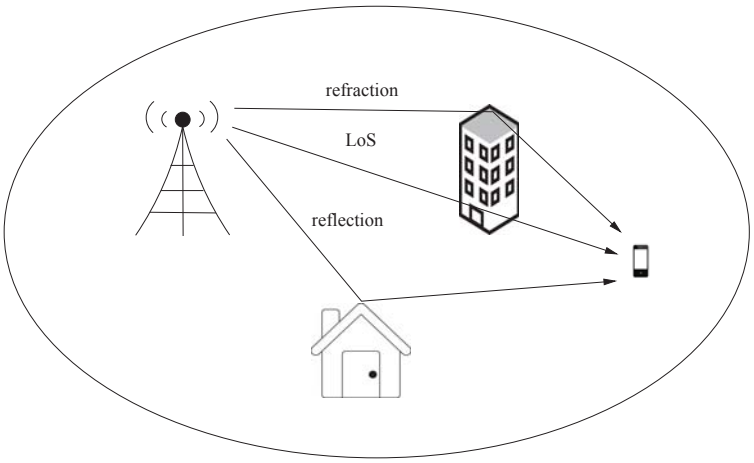

Fig. 1.1. Multipath propagation.

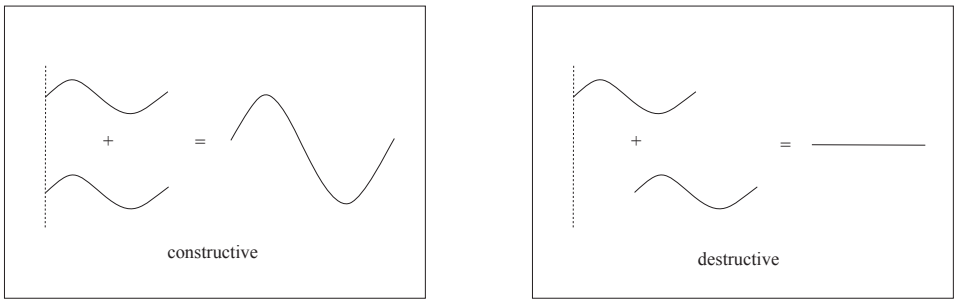

Fig. 1.2. The effect of multipath propagation on received signal.

- Small-Scale Fading

  In addition to the direct wireless connection from the transmitter to the receiver, i.e., the line of sight (LOS), signals can also travel by a number of different propagation paths (Fig. 1.1). Multipath propagation occurs when signals are reflected and diffracted by obstacles, such as buildings, mountains, windows, etc.. Since different signal paths have different phase shifts, signal paths can be combined constructively or destructively at the receiver (Fig. 1.2). The effect of multipath propagation is called small-scale fading.

  The motion of the terminal causes doppler shift. Different signal paths have different doppler shifts and then the frequencies of the signal waves change differently. As a result, the overall wireless channel varies in time. The coherence time T_c is defined as the maximum time interval over which the chan-

nel response is invariant. T_c is inversely proportional to the doppler spread which is the difference between the maximum doppler shift and the minimum doppler shift. A fast fading channel is defined when the coherence time is much shorter than a symbol transmit duration and a slow fading channel is defined when the coherence time is much longer.

A wireless channel also varies in frequency due to the time delay of different paths. The coherence frequency B_c is defined as the range of frequencies over which two frequency components experience correlated magnitude of fading. B_c is inversely proportional to the time delay spread which is the propagation time difference between the longest path and the shortest path. A flat fading channel is defined when B_c is much larger than the signal bandwidth and a frequency-selective fading channel is defined when B_c is much smaller than the signal bandwidth.

Rayleigh fading and Rician fading are two common flat fading channel models. Rayleigh fading is more appropriate to urban areas where LOS propagation is not available. With Rayleigh fading model, the channel response is a complex variable with circularly symmetric complex Gaussian distribution whose mean is 0 and variance is σ^2, denoted as $\mathcal{CN}(0, \sigma^2)$. Its envelop has a Rayleigh distribution with the following probability density function (pdf)

$$p(r) = \frac{r}{\sigma^2} \exp\left(\frac{-r^2}{2\sigma^2}\right).$$

Rician fading channel model is often used when there is a dominant LOS signal. Its envelop has a Rician distribution with the following pdf

$$p(r) = \frac{r}{\sigma^2} \exp\left(-\frac{r^2 + A^2}{2\sigma^2}\right) I_0\left(\frac{Ar}{\sigma^2}\right),$$

where A^2 is the power of the LOS component. $2\sigma^2$ is the average power of the non-LOS multipath components and I_0 is the modified Bessel function of the first kind and zero-order.

- Large-Scale Fading

  Another type of fading is large-scale fading resulting from pass loss and shadowing [2]. Pass loss is the power decay of a radio signal propagating in the environment. The effect of shadowing occurs when the receiver is blocked by tall buildings and then the radio wave is attenuated greatly by going through or around the obstacles (Fig. 1.3).

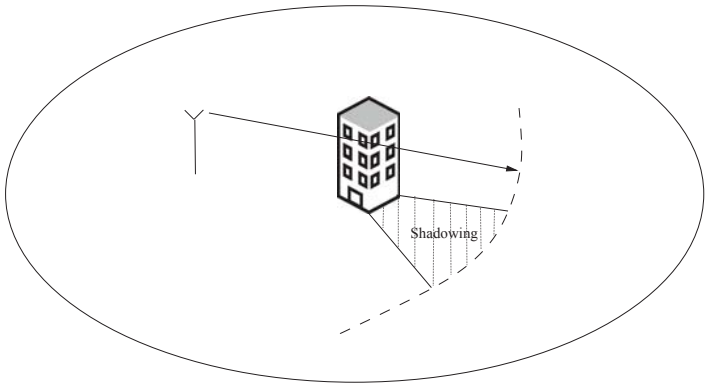

Fig. 1.3. Shadowing effect.

To combat channel fading and achieve high performance in wireless communications, many techniques have been proposed such as diversity techniques and multiplexing techniques [3], [4]. For diversity techniques, a transmitter sends multiple copies of same data via different independent channels. Link reliability is improved by diversity techniques. Multiplexing techniques can improve the data rate of the system by transmitting different data streams across different independent channels.

1.2 Evolution of Cellular Systems

There are many types of services in wireless communications, such as paging systems, broadcasting, wireless local area network (WLAN), cellular systems, satellite communications, etc.. Cellular systems is a very important form of wireless communications. Two-way voice and data communications are supported by cellular systems with regional, national, or international coverage.

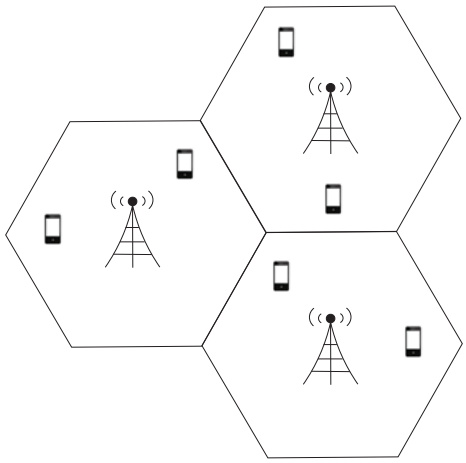

Fig. 1.4. Cellular systems.

In a cellular system, the coverage area is divided into several regular shaped non-overlapping cell such as hexagonal. Each cell is assigned with a base station (BS) which serves the users in the cell (Fig. 1.4). Since the transmit signal power greatly attenuates over some distance, the same set of frequencies can be reused in cells which are far from each other. By the frequency reuse, limited frequency bandwidth is efficiently utilized.

The first generation (1G) cellular systems were introduced in the 1980s which used analog signal radio for communications. The Advance Mobile Phone Service (AMPS) was a 1G system mainly used in North America operating in the 50MHz frequency bands. The spectrum were divided into two parts, one for uplink communications (from users to the BS) and the other for downlink communications (from the BS to users). Poor speech quality was experienced due to the lack of error correction coding in analog communications. The threat of eavesdropping was another problem in 1G systems since little encryption techniques could be implemented on the analog signals.

The second generation (2G) cellular systems, moving from analog to digital, were commercially lunched in the 1990s. Global System for Mobile Communication (GSM) and Interim Standard 95 (IS-95) were the popular 2G standards developed by European Telecommunications Standards Institute (ETSI) and Qualcomm respectively. Especially, GSM [5], [6] operating on the 900MHz or the 1800MHz

bands , was widely used over 219 countries and territories. Time division multiple access (TDMA) technique was utilized for GSM standard, which allows several users to communicate with the BS in the same carrier frequency in different time slots. Evolved 2G systems were also proposed to support data communications other than the voice services [7]. In 1997, the data transmission technology of General Packet Radio Service (GPRS) was integrated into GSM systems, which boosted the date rate up to 114Kbps (kilobit per second). The evolved GSM systems with GPRS was described as 2.5G systems. In 2003, Enhanced Data Rates for GSM Evolution (EDGE) technology was introduced to further improve the date rate up to 384Kbps. And the GSM systems with EDGE was described as 2.75G systems.

As smartphones become widespread and take large worldwide market share of mobile phones, cellular systems needed to be evolved to satisfy huge client demands of data rate both in business and entertainment, such as video calls, games, downloads, mobile TV, etc. Therefore, the third generation (3G) cellular systems, providing much higher data rates, were introduced and widely used in the 2000s. All 3G standards were required to meet the International-Mobile-Telecommunication-2000 (IMT-2000) standard which was established by the International Telecommunication Union (ITU). Universal Mobile Telecommunication System (UMTS) and Code Division Multiple Access 2000 (CDMA2000) were the common 3G systems developed by Third Generation Partnership Project (3GPP) and 3GPP2 (Third Generation Partnership Project 2) respectively. UMTS was based on the GSM system, while CDMA2000 was backward-compatible with 2G IS-95 standard. Most of the UMTS systems in the world adopted Wideband Code Division Multiple Access (W-CDMA) protocols as air interface standard. High Speed Packet Access (HSPA) was an protocol update to UTMS system. HSPA can provide peak data rates of 14.4Mbps (megabit per second) in the downlink and 5.76Mbps in the uplink. The newest evolution of HSPA, Advanced Evolved High Speed Packet Access (Advanced HSPA+), can reach data rate of 84.4Mbps in the downlink and 22 Mbps in the uplink.

In 2008, ITU specified the set of requirements for 4G cellular systems called

IMT-Advanced standard. According to the specifications of IMT-Advanced, 4G systems can provide data rates of 100Mbps for users at high mobility (e.g. cars, trains, etc.) and 1Gbps (gigabit per second) for low mobility communications. Two 4G systems were commercially launched: Mobile Worldwide Interoperability for Microwave Access (Mobile WiMAX) system [8], [9] and Long Term Evolution (LTE) system [10]. Although the initial release of these two standards did not fully comply with IMT-Advanced standard, they were still branded 4G by the service providers. The second versions of mobile WiMAX and LTE, mobile WiMAX Release 2 (also known as 802.16m) and LTE-Advanced respectively, were standardized in 2011, promising the data rate in the order of 1Gbps. Instead of the CDMA technique used in 3G systems, Orthogonal Frequency-Division Multiple Access (OFDMA) is utilized for 4G systems. Another important concept introduced in 4G systems is Multiple-Input Multiple-Output (MIMO) systems, where the BSs and the terminals are equipped with multiple antennas. Due to the extra spatial resources provided by MIMO systems, the link reliability can greatly increase as well as the data rate and power efficiency.

1.3 Next Generation Cellular Systems

A new generation of cellular systems came out about every 10 years since the 1G cellular systems. As 4G systems were commercially deployed in the early 2010s, researchers have started exploring the fifth generation (5G) cellular systems. 5G systems aim to meet the demands of 2020 and beyond.

Requirements for 5G have been discussed by telecommunication companies and research groups. Among the requirements, demands on the number of connections, latency and throughput are mostly mentioned.

- Number of connections

  Although 4G systems have been able to support thousands of connections in a cell, it will not satisfy the connection needs predicted for 2020 due to the huge increase in the popularity of wireless devices, such as smartphones,

tablets, wearable devices, etc.. Therefore, a million connections per square kilometers are expected in 5G. It is envisioned that 5G will provide a fully mobile and connected society [11].

- Latency

  Currently 4G systems have achieved 50ms (millisecond) latency which is a half compared to 3G systems. However, it will not be low enough for future remote control applications such as industrial automation, remote surgery, self-driving car, etc.. Less than 1ms latency is required for 5G to support the services in need of ultra-low latency.

- Throughput

  Lots of new services and new applications rely on high data-rate transmissions, such as 4K video services, virtual reality, cloud storage, etc.. Especially for virtual reality technologies, the throughput is required to be at least 300Mbps which is ten times higher than high-definition (HD) video services. Based on current growth trend, researchers have predicted a 1000-fold increase in data-rate demand by 2020. In 5G, a 10Gbps throughput must be achieved to satisfy such high throughput requirement.

To enable the applications and meet the specifications mentioned above, novel and revolutionary wireless technologies are required. Massive MIMO [12], [13] is one of the most potential technologies for 5G. In massive MIMO systems, the BS is envisioned to be equipped with a very large number of antennas (e.g., hundreds or thousands), while MIMO in 4G only allows 8 antennas at the BS. Huge improvements on the throughput, reliability and energy efficiency can be achieved in massive MIMO systems due to the extra spatial resources provided by the large-scale antenna array. In Section 1.6, more introduction on massive MIMO will be provided. Other promising techniques in 5G developments are millimeter wave (mmWave) technology [14]–[16], device-centric architectures of cellular systems [17], etc..

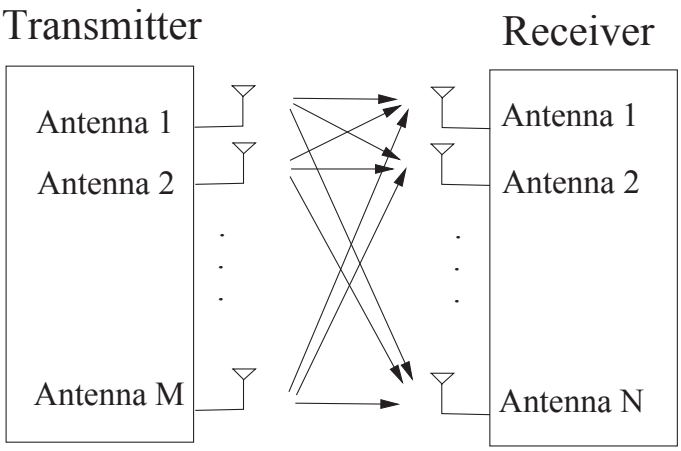

Fig. 1.5. A SU-MIMO system with M transmit antennas and N receive antennas.

1.4 SU-MIMO Systems

MIMO technologies, where the transmitter and the receiver are equipped with multiple antennas, has been applied into 4G. By using the extra spatial resources provided, MIMO systems can achieve great performance in data rate and link reliability without additional cost of bandwidth, transmission time, or power [18]–[21].

MIMO systems can be categorized as single-user MIMO (SU-MIMO) and multi-user MIMO (MU-MIMO). For SU-MIMO systems [22], a single transmitter sends information to a single receiver, as shown in Fig. 1.5. We assume that there are M antennas at the transmitter and N antennas at the receiver. The data intended for the receiver are processed and transformed into the transmit signals to be sent from M BS antennas, which can be mathematically described as an $M \times 1$ signal vector $\mathbf{s}$. If the total average transmit signal power is constrained to be a constant P_t, we have

$$\mathbb{E}[||\mathbf{s}||^2] = P_t,$$

where $||\cdot||$ is the norm operator. The MIMO channel can be mathematically denoted as an $N \times M$ matrix $\mathbf{H}$, where its (i, j)-th entry is the complex channel value from the i-th transmit antenna to the j-th receive antenna. The received signal vector $\mathbf{x}$

at the receiver can be expressed as

$$\mathbf{x} = \mathbf{H}\mathbf{s} + \mathbf{n}, \tag{1.1}$$

where $\mathbf{n}$ is the $N \times 1$ noise vector at the receiver whose entries are independent and identically distributed (i.i.d.) $\mathcal{CN}(0, 1)$ random variables.

When Rayleigh flat fading channels are assumed and the receiver has the knowledge of channel state information (CSI), it has been shown [20] that the capacity of SU-MIMO systems scales linearly with the minimum of the number of transmit antennas and the number of receive antennas, i.e., $\min(M, N)$.

Multiple-input single-output (MISO) systems is a special case for SU-MIMO systems where the receiver is equipped with one single antenna, i.e., $N = 1$. Then the vector $\mathbf{x}$ and the vector $\mathbf{n}$ in (1.1) reduce to complex values (x and n). The channel matrix $\mathbf{H}$ reduces to a $1 \times M$ vector $\mathbf{h}$. The received signal at the receiver in MISO systems can be represented as

$$x = \mathbf{h}\mathbf{s} + n. \tag{1.2}$$

To measure the performance of the transmission, an important criterion is the signal-to-noise-ratio (SNR), defined as the signal power divided by the noise variance. In our model, since the noise variance is normalized, we have

$$\mathrm{SNR} = ||\mathbf{h}\mathbf{s}||^2.$$

The achievable rate for the SU-MISO system is given by

$$R = \log_2(1 + \mathrm{SNR}) = \log_2(1 + ||\mathbf{h}\mathbf{s}||^2).$$

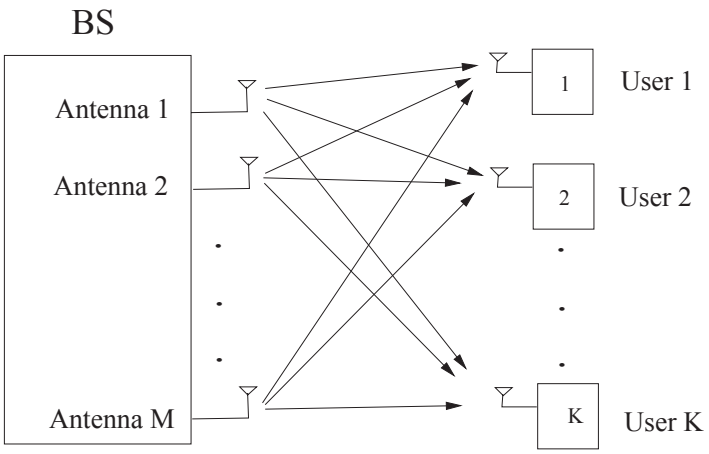

Fig. 1.6. MU-MIMO downlink with M BS antennas and K users.

1.5 MU-MIMO systems

For MU-MIMO systems [23]–[25], one multiple-antenna BS serves multiple users simultaneously. As shown in Fig. 1.6, the BS equipped with M antennas serves K single-antenna users. The K user data signals are processed and transformed into an $M \times 1$ signal vector $\mathbf{s}$ which is to be transmitted from the M BS antennas. $\mathbf{s}$ contains the information for all K users. Define P_t as the average total transmit power, then we have

$$\mathbb{E}[||\mathbf{s}||^2] = P_t.$$

The wireless channels from the BS to the K users can be mathematically described as a $K \times M$ matrix $\mathbf{H}$, where its (i, j)-th entry is the complex channel value from the i-th BS antenna to the j-th user.

Denote the received signal at User k by x_k and the noise signal at User k by n_k. The channel vector from the BS to User k is defined as $\mathbf{h}_k$ and then $\mathbf{H}$ can be

written as

$$\mathbf{H} = \begin{bmatrix} \mathbf{h}_1 \\ \mathbf{h}_2 \\ \vdots \\ \mathbf{h}_K \end{bmatrix}.$$

The received signal at User k, x_k, is given by

$$x_k = \mathbf{h}_k \mathbf{s} + n_k. \tag{1.3}$$

Define $\mathbf{x}$ as the $K \times 1$ received signal vector for all K users, then we have

$$\mathbf{x} = \begin{bmatrix} x_1 \\ x_2 \\ \vdots \\ x_K \end{bmatrix}.$$

Based on (1.3), the $K \times 1$ received signal vector $\mathbf{x}$ is given by

$$\mathbf{x} = \mathbf{H}\mathbf{s} + \mathbf{n} \tag{1.4}$$

where $\mathbf{n}$ is the noise signal vector and its n-th entry is n_k. It was proved in [20] that the sum capacity of MU-MIMO system grows linearly with the minimum of the number of BS antennas and the number of users, i.e., $\min(M, K)$.

Equation (1.3) shows that the transmission from the BS to User k in MU-MIMO has a similar structure to the MISO transmission. However, there is a fundamental difference between the two systems. The signal vector $\mathbf{s}$ in MU-MIMO contains the information for all K users, while the signal vector $\mathbf{s}$ in MISO systems is for a single user. Then in addition to the desired signal and noise, each user in MU-MIMO systems also receives inter-user interference (i.e., signals intended for other users) which attenuates the performance of its own communication.

To improve the system performance and reduce user-interference effect, precod-

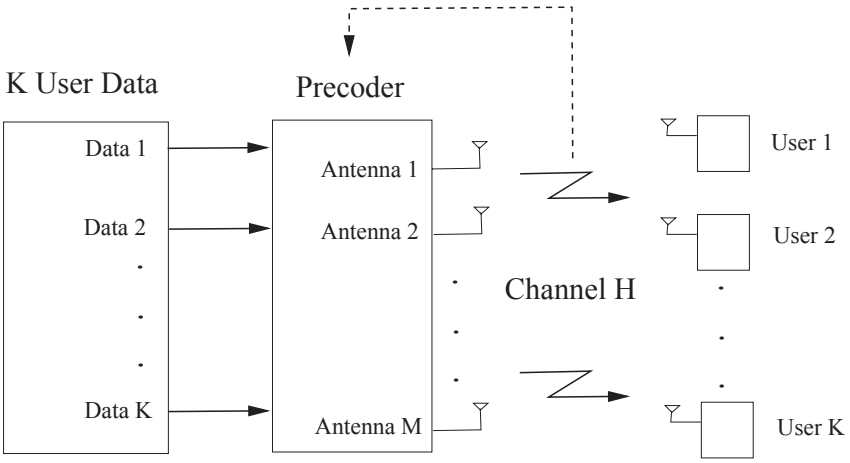

Fig. 1.7. MU-MIMO downlink with precoding.

ing can be used at the BS for the downlink transmission when the CSI is available at the transmit side. Precoding is a signal processing technique which utilizes the CSI to process and transform the data signals (intended for the users) into signals to be sent by the multiple BS antennas (Fig. 1.7). Precoding can be categorized as non-linear precoding and linear precoding [26]. Although non-linear precoding, such as dirty paper coding (DPC), can achieve channel capacity, its high complexity is a great challenge in practical applications. Here we discuss linear precoding schemes which can achieve reasonable performance with manageable complexity.

Define $\mathbf{q}$ as the $K \times 1$ data signal vector, where the k-th entry q_k is the signal to be transmitted to User k. Assume that all entries of $\mathbf{q}$ are independent of each other and normalized to 1, i.e., $\mathbb{E}[|q_k|^2] = 1$. Linear precoding can be represented by an $M \times K$ matrix, denoted as $\mathbf{W}$. Via multiplication by $\mathbf{W}$, the input signal vector $\mathbf{q}$ is transformed into the $M \times 1$ precoded signal vector $\mathbf{s}$, shown as

$$\mathbf{s} = \sqrt{p}\mathbf{W}\mathbf{q}, \tag{1.5}$$

where p is a coefficient for the average transmit power constraint. Let P_t be the average transmit power, from (1.5) we have

$$p\mathbb{E}[||\mathbf{W}\mathbf{q}||^2] = P_t. \tag{1.6}$$

Since each entry of $\mathbf{q}$ is normalized and independent, we have

$$\mathbb{E}[\mathbf{q}\mathbf{q}^H] = \mathbf{I}_K$$

where $\mathbf{I}_K$ is the $K \times K$ identity matrix. Then the coefficient p can be calculated to be

$$p = \frac{P_t}{\mathbb{E}[||\mathbf{W}\mathbf{q}||^2]} = \frac{P_t}{\mathbb{E}[\mathrm{tr}\,(\mathbf{W}\mathbf{W}^H)]} \tag{1.7}$$

The received signal vector $\mathbf{x}$ is given by

$$\mathbf{x} = \sqrt{p}\mathbf{H}\mathbf{W}\mathbf{q} + \mathbf{n}. \tag{1.8}$$

The received signal at User k in (1.3) can be rewritten as

$$\begin{aligned} x_k &= \sqrt{p}\mathbf{h}_k\mathbf{W}\mathbf{q} + n_k \\ &= \sqrt{p}\mathbf{h}_k\mathbf{w}_k q_k + \sqrt{p}\sum_{j=1, j\neq k}^{K} \mathbf{h}_k\mathbf{w}_j q_j + n_k, \end{aligned} \tag{1.9}$$

where $\mathbf{w}_k$ is the kth column of the precoding matrix $\mathbf{W}$. The first term in (1.9) contains the desired signal. The second term shows the inter-user interference containing the information for other users and the third term is the noise.

To measure the performance of the transmission with interference, an important criterion is the signal-to-interference-plus-noise-ratio (SINR), defined as the desired signal power divided by the sum of the interference power and the noise variance. In our model, the SINR at User k can be calculated to be [27]

$$\mathrm{SINR}_k = \frac{p|\mathbf{h}_k\mathbf{w}_k|^2}{1 + p\sum_{j=1, j\neq k}^{K} |\mathbf{h}_k\mathbf{w}_j|^2}.$$

The achievable rate for User k is given by

$$R_k = \log_2(1 + \mathrm{SINR}_k),$$

and the sum-rate of the MU-MIMO downlink is

$$R_{\text{sum}} = \sum_{k=1}^{K} \log_2(1 + \text{SINR}_k).$$

There are four common linear precoding schemes which are maximum-ratio-transmit (MRT) precoding, zero-forcing (ZF) precoding, regularized zero-forcing (RZF) precoding and wiener filter (WF) precoding. In what follows, these linear precoding schemes are briefly introduced.

- MRT precoding

  MRT precoding [26], [28], also called matched-filter (MF) precoding, maximizes the sum of K users' SNRs. Each column vector $\mathbf{w}_k$ ($k = 1, 2, \cdots, K$) of the MRT precoding matrix $\mathbf{W}$ is derived by maximizing the following sum of the ratios [26], shown as

$$(\mathbf{w}_{1,\text{MRT}}, \mathbf{w}_{2,\text{MRT}}, \cdots, \mathbf{w}_{K,\text{MRT}}) = \underset{\mathbf{w}_1, \mathbf{w}_2, \cdots, \mathbf{w}_K}{\text{argmax}} \sum_{k=1}^{K} \frac{\mathbb{E}\left[\left|\sqrt{p_{\text{MRT}}}\mathbf{h}_k \mathbf{w}_k q_k\right|^2\right]}{\mathbb{E}[|n_k|^2]}$$
$$\text{s.t. } \mathbb{E}\left[\left|\left|\sqrt{p_{\text{MRT}}} \sum_{k=1}^{K} \mathbf{w}_k q_k\right|\right|^2\right] = P_t,$$

  where $(\cdot)^H$ denotes the Hermitian matrix. Since the noise power is normalized to 1, i.e., $\mathbb{E}[|n_k|^2] = 1$, MRT precoding equivalently maximizes the sum of each user's desired signal power under the transmit power constraint. According to the Cauchy-Schwarz inequality, the solution is given by

$$\mathbf{w}_{k,\text{MRT}} = \mathbf{h}_k^H$$

  and then MRT precoding matrix $\mathbf{W}$ is given by

$$\begin{aligned} \mathbf{W}_{\text{MRT}} &= \begin{bmatrix} \mathbf{w}_{1,\text{MRT}} & \mathbf{w}_{2,\text{MRT}} & \cdots & \mathbf{w}_{K,\text{MRT}} \end{bmatrix} \\ &= \begin{bmatrix} \mathbf{h}_1^H & \mathbf{h}_2^H & \cdots & \mathbf{h}_K^H \end{bmatrix} \\ &= \mathbf{H}^H \end{aligned}$$

From (1.7), the coefficient p_{MRT} can be calculated to be

$$p_{\mathrm{MRT}} = \frac{P_t}{\mathbb{E}[\mathrm{tr}(\mathbf{H}^H\mathbf{H})]}.$$

The SINR for User k is

$$\mathrm{SINR}_k = \frac{p_{\mathrm{MRT}}|\mathbf{h}_k\mathbf{h}_k^H|^2}{1 + p_{\mathrm{MRT}}\sum_{j=1,j\neq k}^{K}\left|\mathbf{h}_k\mathbf{h}_j^H\right|^2}.$$

While MRT precoding maximizes the desired signal power [26], the interference elimination is not taken into consideration in the precoding design. As a result, the performance of MRT precoding is largely limited by the effect of interference, even for high SNR.

- ZF precoding and RZF precoding

  ZF precoding [29] aims to completely remove the user-interference. If the product of the channel matrix $\mathbf{H}$ and the precoding matrix $\mathbf{W}$ is an identity matrix, shown as

  $$\mathbf{HW} = \mathbf{I}_K, \tag{1.10}$$

  the received signal vector $\mathbf{x}$ in (1.8) can be rewritten as

  $$\mathbf{x} = \sqrt{p}\mathbf{q} + \mathbf{n}$$

  and the received signal at User k is given by

  $$x_k = \sqrt{p}q_k + n_k.$$

  It can be clearly observed that each user contains only the desired signal and the noise signal while the user-interference is completely removed.

ZF precoding matrix was derived [26] as

$$\mathbf{W}_{\mathrm{ZF}} = \mathbf{H}^H \left(\mathbf{H}\mathbf{H}^H\right)^{-1}, \tag{1.11}$$

which is the pseudoinverse of the channel matrix $\mathbf{H}$. From (1.7), the coefficient p_{ZF} is given by

$$p_{\mathrm{ZF}} = \frac{P_t}{\mathbb{E}\left[\mathrm{tr}((\mathbf{H}\mathbf{H}^H)^{-1})\right]}.$$

The SNR at User k with ZF precoding is

$$\mathrm{SNR}_k = p_{\mathrm{ZF}}.$$

Thus the sum-rate with ZF precoding depends on the condition of the channel inverse $(\mathbf{H}\mathbf{H}^H)^{-1}$. When $\mathbf{H}$ is poorly conditioned, the singular value spread of $\mathbf{H}$ (i,e,. the ratio of the maximum singular value to the minimum singular value of $\mathbf{H}$) is large [26], [30]. It is shown in [31], [32] that the large singular value spread leads to poor performance of ZF precoding.

RZF precoding, as a generalization of ZF precoding, is proposed to regularize ZF precoding matrix. It is given by

$$\mathbf{W}_{\mathrm{RZF}} = \mathbf{H}^H(\mathbf{H}\mathbf{H}^H + c\mathbf{I}_K)^{-1}, \tag{1.12}$$

where $c > 0$ is a constant.

By adding a scaled version of the identity matrix before inverting, RZF precoding can improve the behavior of the inverse in (1.12) no matter how poor the condition of $\mathbf{H}$ is. However, the interference increases as c increases. So it is reasonable to use SINR as a metric to determine c. In [31], SINR is achieved by dividing the average power of the desired signal by the average power of the interference and the noise. As a result, the SINR at each user is independent of user index k and c can be determined by maximizing the

SINR. [31] shows that the sum-rate of RZF precoding approaches the sum capacity for low SNR with the assumption of Rayleigh fading channel and $K = M$. For high SNR, the sum-rate of RZF precoding approaches the sum-rate of ZF precoding.

- WF precoding

  Mean square error (MSE) measures the difference between the received signal and the input signal. WF precoding [33], [34], also called minimum-mean-square-error (MMSE) precoding, is designed by minimizing the MSE under the transmit power constraint. The precoding design problem can be represented as

$$(\mathbf{W}_{\mathrm{WF}}, \beta) = \underset{\mathbf{W},\beta}{\operatorname{argmin}} \mathbb{E}[||\mathbf{q} - \beta^{-1}\mathbf{x}||^2] \quad \text{s.t.: } \mathbb{E}[||\sqrt{p}\mathbf{W}\mathbf{q}||^2] = P_t$$

  where β is a coefficient of the SNR to be optimized for minimizing the MSE. The solution is given by

$$\mathbf{W}_{\mathrm{WF}} = \beta \left(\mathbf{H}^H\mathbf{H} + \frac{K}{P_t}\mathbf{I}_M \right)^{-1} \mathbf{H}^H.$$

  and

$$\beta = \sqrt{\frac{P_t}{\mathrm{tr}\left(\left(\mathbf{H}^H\mathbf{H} + \frac{K}{P_t}\mathbf{I}_M \right)^{-2} \mathbf{H}^H\mathbf{H} \right)}}.$$

  From (1.7), we have

$$p_{\mathrm{WF}} = \frac{P_t}{\mathbb{E}[\mathrm{tr}(\mathbf{W}_{\mathrm{WF}}\mathbf{W}_{\mathrm{WF}}^H)]}.$$

  Since

$$\mathbb{E}[\mathrm{tr}(\mathbf{W}_{\mathrm{WF}}\mathbf{W}_{\mathrm{WF}}^H)] = \mathbb{E}\left[\beta^2 \mathrm{tr}\left(\left(\mathbf{H}^H\mathbf{H} + \frac{K}{P_t}\mathbf{I}_M \right)^{-2} \mathbf{H}^H\mathbf{H} \right) \right] = P_t,$$

the power constraint coefficient is calculated to be 1, i.e., $p_{\mathrm{WF}} = 1$.

It is observed that when $K/P_t \to 0$, WF precoding converges to ZF precoding. When $K/P_t \to \infty$, WF precoding converges to MRT precoding.

It was shown in [26] that with Rayleigh flat fading channel, ZF precoding performs better than MRT precoding at high SNR. It is because that the interference limits the performance of MRT precoding. However, at low SNR, ZF precoding is outperformed by MRT precoding. By minimizing the MSE, WF precoding makes a balance between the desired signal power maximization in MRT precoding and the interference elimination in ZF precoding.

1.6 Massive MIMO Systems

Massive MIMO [12], [13], [35], [36], also known as very large MIMO or large-scale antenna systems, is one of the most promising technologies for the next generation cellular systems. It is envisioned [13] that in massive MIMO, the BS is equipped with hundreds of antennas and serves tens of users at the same time. With excess spatial resources, massive MIMO can achieve all the merits of MIMO systems with a much greater scale.

As the number of transmit antennas goes large, there are new phenomenons in massive MIMO compared to conventional MIMO. Under independent Rayleigh flat fading channel, the channel vectors from the BS to the individual users approach orthogonal as the number of transmit antennas goes to infinity [37]. Recall that the channel vector from the BS to User k is denoted by $\mathbf{h}_k$ and the number of BS antennas is denoted by M. We have

$$\frac{1}{M}\mathbf{h}_k\mathbf{h}_j^H \xrightarrow{a.s.} 0, \quad \text{as } M \to \infty.$$

where $\xrightarrow{a.s.}$ denotes the almost surely convergence. Due to the asymptotic orthogonality of the channel vectors, MRT precoding is expected to have good performance in massive MIMO since the interference diminishes when the number of antennas

approaches infinity and the desired signal power is still maximized. As mentioned in Section 1.5, the BS needs the knowledge of the downlink CSI for precoding. The downlink CSI acquisition method in massive MIMO is different to conventional MIMO [13]. In LTE standard, downlink training is used for the CSI acquisition. However, this method is not feasible for massive MIMO since the complexity of downlink training scales with the number of BS antennas. In massive MIMO, time division duplex (TDD) scheme can be used where the uplink transmission and the downlink transmission use the same frequency band while they are separated by different time slots. In TDD scheme, there is a possibility to obtain channel reciprocity (i.e., the downlink channel matrix equals to the transpose of the uplink channel matrix). Then the downlink CSI can be achieved by uplink traning in which the complexity of uplink training scales as the number of users. In massive MIMO, pilot contamination [37]–[39] is a big issue when a multi-cell massive MIMO system is investigated. Pilot contamination occurs when non-orthogonal pilots are used during the uplink training. The channel estimate between the BS and the targeted user is polluted by the channel information of the users who transmit the pilot that is non-orthogonal to the pilot of the targeted user .

Massive MIMO is a new research field for wireless communications. The way of analyzing and designing a massive MIMO system is very different to that in a traditional MIMO system.

1.7 Thesis Contributions and Outline

As a new technology in wireless communications, performance analysis on massive MIMO is an essential research aspect. Due to the huge demands of data rate in current and future wireless systems, most work on performance analysis focus on the sum-rate performance of massive MIMO in different scenarios. By assuming that both M and K go to infinity with a fixed ratio, existing work use the asymptotic deterministic equivalence to achieve the deterministic SINR expression and then the sum-rate result. But, in practical scenarios, the number of users K is limited.

The number of BS antennas is large in massive MIMO, but limited as well. This motivates us to analyze the sum-rate performance of massive MIMO within moderate number of users and large but limited number of BS antennas. We derive the sum-rate of massive MIMO by a different method to existing work, via analysis on the statistical behavior of the SINR.

Moreover, other quality-of-service (QoS) measures, e.g. outage probability, are also important for wireless systems. For massive MIMO, even though the theoretical system sum-rate is shown to increase with more users, if individual users undergo high outage probabilities, the real throughput of the system can be low. This motivates us to conduct an outage probability analysis of massive MIMO.

In addition, we also propose a modified MRT precoding scheme that works when the system has per-antenna power constraint. Antenna transmit power is an important factor for massive MIMO transceiver designs. For the system downlink, while several precoding schemes have been widely used, such as MRT, ZF, and WF, they consider a total average power constraint across all BS antennas. However, in practical systems, each antenna at the BS is equipped with an individual power amplifier with its limited effective operation interval. Thus each antenna has its own power constraint. It is therefore more practical to consider the per-antenna power constraint in addition to the total transmit power constraint in the precoding design.

The details of the contributions of the thesis is explained as follows:

- In this thesis, we study the outage probability analysis for massive MIMO systems. While the sum-rate is a fundamental performance measure for massive MIMO, other measures such as the outage probability is also important in evaluating the quality-of-service (QoS) experienced by the users. For massive MIMO systems, even though the theoretical system sum-rate can increase with more users, an excessively large number of users can result in very low user SINR, which is undesirable for both carriers and customers.

- Existing work rely on the asymptotic deterministic equivalence to obtain an

accurate deterministic SINR expression. However, the outage probability can not be derived this way. In this thesis, we preserve the random nature of the SINR and derive an analytical expression of outage probability.

- In the analysis, we derive the distribution of the interference power with the help of central limit theory and existing result on the distribution of sum of correlated Gamma variables. The pdf of the interference power is first shown in an infinite summation form, and then simplified into a closed-form for further analysis. The outage probability and the sum-rate for the massive MIMO are derived from the interference analysis and observations on the variances of different terms of the SINR.

- From the simulations, we observe that for a massive MIMO system with a large but finite number of antennas, the outage probability increases rapidly to 1 even for moderate number of users (e.g., $15 < K < 20$). This shows that outage probability analysis is necessary for massive MIMO performance.

- We propose a modified MRT precoding under per-antenna power constraint. The outage probability and the sum-rate formulas are derived following similar method proposed in the former work. From the simulations, it can be shown that the modified MRT precoding can achieve a better performance in both outage probability and sum-rate than the conventional MRT precoding, even with more strict power constraint.

The remainder of the thesis is organized as follows. Chapter 2 analyzes the outage probability and the sum-rate for massive MIMO downlink with MRT precoding. Chapter 3 extends the work to systems with per-antenna power constraint and a modified MRT precoding is proposed. Chapter 4 draws the conclusions and discusses on the possible future work based on this thesis.

Chapter 2

Performance Analysis of Massive MIMO Under MRT Precoding

In this chapter, we work on the performance analysis of massive MIMO downlink under MRT precoding. We first study the distribution of the interference power of the multi-user communications and achieve its pdf in closed-form. By using the pdf formula, the outage probability and the sum-rate of the system are both investigated. Simulations show that for a massive MIMO system with large but finite number of antennas, while the sum-rate of the system increases as the number of users increases, the outage probability increases rapidly to 1 even for moderate number of users. This reflects the importance of the outage probability analysis.

2.1 Background and Related Work

There are many papers on performance analysis of massive MIMO. In [12], the performance is studied for both single-cell and multi-cell massive MIMO. Rayleigh flat fading channel is assumed in single-cell massive MIMO donwlink while Rayleigh fading and large-scale fading are both considered in multi-cell massive MIMO dowlink. It is also assumed that the number of antennas M and the number of single-antenna users K go to infinity, while the ratio of K/M is fixed. The SINR with ZF precoding is investigated when perfect CSI is assumed at the BS. Both per-

fect CSI and imperfect CSI are considered for the SINR with MRT precoding. By the asymptotic deterministic equivalences, the deterministic SINR expressions are derived. In [40], asymptotically tight approximations of the downlink achievable rates with MRT precoding and RZF percoding are derived. A multi-cell system with imperfect CSI, channels with correlation and path loss is considered. It is assumed that the number of antennas goes to infinity while the number of users is finite. Assuming that the users know the expectations of channel random variables, an unique SINR expression based on the techniques developed in [39] is provided. As the number of antennas goes infinity, the asymptotic deterministic equations are used to approximate the interference power of the SINR as deterministic and then the analytical results of SINR and achievable rate are achieved. In [41], the downlink sum-rate performance of ZF and RZF precoding in a single-cell network is studied. Imperfect CSI and per-user channel correlation are considered. It is also assumed that the number of single-antenna users and the number of BS antennas approach infinity, but with a fixed ratio. In the derivation, a deterministic equivalent of the empirical Stieltjes transform of large random matrices is used to achieve the deterministic SINR approximations and the deterministic sum-rate approximations. By maximizing the sum-rate, the regularization parameter for RZF is derived and the optimal power allocation schemes for both ZF and RZF are derived. In [42], a single-cell multi-user massive MIMO system under Rayleigh flat fading channel is considered. Imperfect CSI at the BS is assumed. Through a Bayesian approach, capacity lower bounds of MRT precoding and ZF precoding are derived. It is shown in [42] that ZF precoding outperforms MRT precoding for high spectral-efficiency and low energy-efficiency, while MRT precoding performs better than ZF precoding at low spectral-efficiency and high energy-efficiency. In [43], a single-cell two-user massive MIMO downlink is considered. It is assumed that the channels from the BS to the users are correlated and the BS has perfect CSI. By the law of large numbers, the Gram matrix associated with the channel matrix is approximated as deterministic. The analytical result of the sum-rate is derived using the deterministic Gram matrix. The optimal user power allocation scheme is derived by maximizing the

sum-rate. In [44], a point-to-point massive MIMO is considered. Three scenarios are discussed as follows: 1) large number of transmit antennas M and moderate number of receive antenna N; 2) large N and moderate M; 3) large M and large N with fixed ratio of M/N. Rayleigh flat fading is considered. It is assumed that the transmitter does not have the knowledge of channel information. By using central limit theory, the distribution of the achievable rate is asymptotically approximated as Gaussian. Then the outage probability is approximated using the Q-function.

2.2 System Model

We consider a single-cell multi-user massive MIMO system which has a BS and K single-antenna users (Fig. 2.1). The BS is equipped with M antennas where M is assumed to be very large ($M \gg 1$), e.g., a few hundreds [13], [37]. Rayleigh flat fading channels are considered. Let $\mathbf{H}$ be the $K \times M$ channel matrix and $\mathbf{h}_k$ is the $1 \times M$ channel vector from the BS antennas to the kth user. Entries of $\mathbf{H}$ are distributed as i.i.d. $\mathcal{CN}(0, 1)$. We assume that the BS has perfect downlink CSI. As mentioned in Section 1.6, this can be achieved when TDD scheme is used and channel reciprocity holds. If the BS can accurately estimate the uplink channel by uplink training, the downlink channel can be achieved using channel reciprocity.

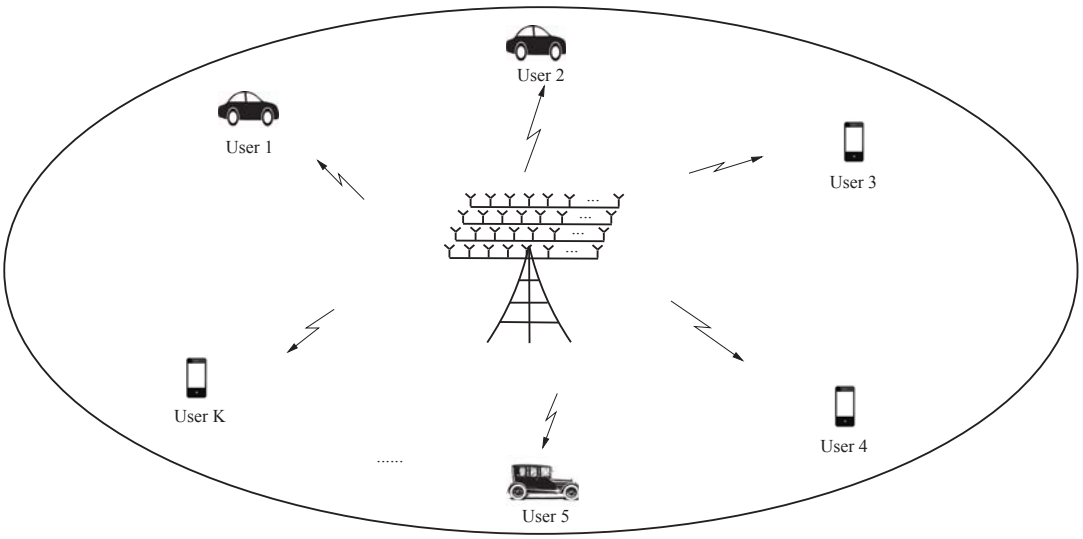

Fig. 2.1. Single-cell massive MIMO with Rayleigh fading.

Let $\mathbf{q}$ be the $K \times 1$ symbole vector. q_k is the symbol for User k and independent of q_j ($j = 1, 2, \cdots, K$, $j \neq k$). The power of each data symbol is normalized to 1, i.e.,

$$\mathbb{E}\left[|q_k|^2\right] = 1.$$

In our work, MRT precoding is considered. Notice that in massive MIMO systems, ZF precoding and WF precoding have high computational complexity due to the channel inverse, while MRT precoding has low-complexity and good asymptotic performance (as mentioned in Chapter 1). With MRT precoding, the transmit signal vector from the BS to all users is

$$\begin{aligned}\mathbf{s} &= \sqrt{\alpha}\mathbf{H}^H\mathbf{q} \\ &= \sqrt{\alpha}\sum_{k=1}^{K}\mathbf{h}_k^H q_k,\end{aligned}$$

where α is a coefficient used for total average transmit power constraint. Define P_t as the average total transmit power. We need

$$\mathbb{E}[||\mathbf{s}||^2] = P_t$$

Since Rayleigh flat fading is assumed, the coefficient α can be calculated to be

$$\alpha = \frac{P_t}{\mathbb{E}[\mathrm{tr}(\mathbf{H}^H\mathbf{H})]} = \frac{P_t}{KM}.$$

The received signal vector $\mathbf{x}$ is

$$\mathbf{x} = \sqrt{\frac{P_t}{KM}}\mathbf{H}\mathbf{H}^H\mathbf{q} + \mathbf{n} \tag{2.1}$$

where $\mathbf{n}$ is the noise vector whose entries are distributed as $\mathcal{CN}(0, 1)$. Equation

(2.1) can be rewritten as

$$\begin{bmatrix} x_1 \\ x_2 \\ \vdots \\ x_k \end{bmatrix} = \sqrt{\frac{P_t}{KM}} \begin{bmatrix} \mathbf{h}_1\mathbf{h}_1^H & \mathbf{h}_1\mathbf{h}_2^H & \cdots & \mathbf{h}_1\mathbf{h}_K^H \\ \mathbf{h}_2\mathbf{h}_1^H & \mathbf{h}_2\mathbf{h}_2^H & \cdots & \mathbf{h}_2\mathbf{h}_K^H \\ \vdots & \vdots & \ddots & \vdots \\ \mathbf{h}_K\mathbf{h}_1^H & \mathbf{h}_K\mathbf{h}_2^H & \cdots & \mathbf{h}_K\mathbf{h}_K^H \end{bmatrix} \cdot \begin{bmatrix} q_1 \\ q_2 \\ \vdots \\ q_k \end{bmatrix} + \begin{bmatrix} n_1 \\ n_2 \\ \vdots \\ n_k \end{bmatrix}$$

where n_k is the kth entry of $\mathbf{n}$. Then the received signal at the kth user is given by

$$\begin{aligned} x_k &= \sqrt{\frac{P_t}{KM}} \sum_{i=1}^{K} \mathbf{h}_k \mathbf{h}_i^{\mathrm{H}} q_i + n_k \\ &= \sqrt{\frac{P_t}{KM}} \mathbf{h}_k \mathbf{h}_k^{\mathrm{H}} q_k + \sqrt{\frac{P_t}{KM}} \sum_{j=1, j\neq k}^{K} \mathbf{h}_k \mathbf{h}_j^{\mathrm{H}} q_j + n_k. \end{aligned} \tag{2.2}$$

The first term in (2.2) represents the desired signal component for User k, and the second term is the user-interference. The SINR of User k can be calculated to be

$$\begin{aligned} \mathrm{SINR}_k &= \frac{\left| \sqrt{\frac{P_t}{KM}} \mathbf{h}_k \mathbf{h}_k^H q_k \right|^2}{\mathrm{Var}(n_k) + \left| \sqrt{\frac{P_t}{KM}} \sum_{j=1, j\neq k}^{K} \mathbf{h}_k \mathbf{h}_j^H q_j \right|^2} \\ &= \frac{\frac{P_t}{KM} \left| \mathbf{h}_k \mathbf{h}_k^H q_k \right|^2}{1 + \frac{P_t}{KM} \sum\limits_{j=1, j\neq k}^{K} |\mathbf{h}_k \mathbf{h}_j^H q_j|^2 + \frac{P_t}{KM} \sum\limits_{m=1, m\neq k}^{K} \sum\limits_{n=1, n\neq k, n\neq m}^{K} |\mathbf{h}_k \mathbf{h}_m^H q_m q_n^H \mathbf{h}_n \mathbf{h}_k^H|}. \end{aligned}$$

Recall that the data signal $\{q_k\}_{k=1}^K$ is distributed as i.i.d. $\mathcal{CN}(0, 1)$, we have

$$\begin{aligned} &\mathbb{E}\left[|q_k|^2\right] = 1, \qquad k = 1, 2, \cdots, K. \\ &\mathbb{E}\left[\left|q_k q_j^H\right|\right] = 0, \quad k \neq j. \end{aligned}$$

Then the SINR of User k is given by (averaged over $\mathbf{q}$)

$$\mathrm{SINR}_k = \frac{\frac{P_t}{KM} |\mathbf{h}_k \mathbf{h}_k^H|^2}{1 + \frac{P_t}{KM} \sum_{j=1, j\neq k}^{K} \left| \mathbf{h}_k \mathbf{h}_j^H \right|^2}. \tag{2.3}$$

To understand the performance of the massive MIMO system, we analyze the

statistical properties of SINR_k. Especially, the statistical properties of the interference term in the denominator of (2.3) are crucial.

2.3 Analysis on Interference Power

In this section, we analyze the user-interference. Instead of using asymptotic results by deterministic equivalence to find the average interference power, we study its random behaviour and derive a closed-form approximation of its pdf. Discussions on the properties of the pdf are also provided.

To help the presentation, we use Y_k to denote the power of the interference experienced by User k, i.e.,

$$Y_k \triangleq \frac{1}{M} \sum_{j=1, j\neq k}^{K} |\mathbf{h}_k \mathbf{h}_j^{\mathrm{H}}|^2.$$

The following proposition is proved.

Proposition 1. *Define*

$$\eta = \frac{K-1}{\sqrt{M}+K-2}. \tag{2.4}$$

When $M \gg 1$, the pdf of Y_k has the following approximation:

$$f_{Y_k}(y) \approx \tilde{f}_{Y_k}(y) = (1-\eta) \sum_{i=0}^{\infty} \eta^i \phi\left(y; K+i-1, 1-\frac{1}{\sqrt{M}}\right), \tag{2.5}$$

where $\phi(y;\alpha,\beta) = \frac{y^{\alpha-1}e^{-y/\beta}}{\beta^\alpha(\alpha-1)!}, y>0$ is the pdf of Gamma distribution with shape parameter α and scale β.

Proof. When $M \to \infty$, from the Lindeberg-Lévy central limit theorem, we have

$$\frac{1}{\sqrt{M}} \mathbf{h}_k \mathbf{h}_j^H \xrightarrow{d} \mathcal{CN}(0,1) \quad k \neq j,$$

where $\xrightarrow{d}$ means convergence in distribution. Then $\frac{1}{M}|\mathbf{h}_k \mathbf{h}_j^H|^2$ converges to Gamma distribution $\phi(y;1,1)$. Next we calculate the correlation coefficient ρ_{jl} of $\frac{1}{M}|\mathbf{h}_k \mathbf{h}_j^H|^2$

and $\frac{1}{M}|\mathbf{h}_k\mathbf{h}_l^H|^2$ for $j \neq l$, defined as

$$\rho_{jl} = \frac{\mathrm{cov}\left(\frac{1}{M}|\mathbf{h}_k\mathbf{h}_j^H|^2, \frac{1}{M}|\mathbf{h}_k\mathbf{h}_l^H|^2\right)}{\sqrt{\mathrm{Var}\left\{\frac{1}{M}|\mathbf{h}_k\mathbf{h}_j^H|^2\right\}\mathrm{Var}\left\{\frac{1}{M}|\mathbf{h}_k\mathbf{h}_l^H|^2\right\}}}. \tag{2.6}$$

The numerator (the covariance) is calculated as

$$\begin{aligned} & \mathrm{cov}\left(\frac{1}{M}|\mathbf{h}_k\mathbf{h}_j^H|^2, \frac{1}{M}|\mathbf{h}_k\mathbf{h}_l^H|^2\right) \\ = \; & \mathbb{E}\left[\frac{1}{M}|\mathbf{h}_k\mathbf{h}_j^H|^2\frac{1}{M}|\mathbf{h}_k\mathbf{h}_l^H|^2\right] - \mathbb{E}\left[\frac{1}{M}|\mathbf{h}_k\mathbf{h}_j^H|^2\right]\mathbb{E}\left[\frac{1}{M}|\mathbf{h}_k\mathbf{h}_l^H|^2\right] \\ = \; & \mathbb{E}\left[\frac{1}{M^2}\mathbf{h}_k\mathbf{h}_j^H\mathbf{h}_j\mathbf{h}_k^H\mathbf{h}_k\mathbf{h}_l^H\mathbf{h}_l\mathbf{h}_k^H\right] - 1 \end{aligned}$$

Since the channel vectors $\mathbf{h}_i$ for $i = 1, 2, \cdots, K$ are independent from each other, we can first calculate the average of $\mathbf{h}_j^H\mathbf{h}_j$ and $\mathbf{h}_l^H\mathbf{h}_l$ in the first term. Recall that Rayleigh flat fading channel is assumed and then $\mathbb{E}[\mathbf{h}_i^H\mathbf{h}_i] = \mathbf{I}_M$ for $i = 1, 2, \cdots, K$. So we have

$$\mathrm{cov}\left(\frac{1}{M}|\mathbf{h}_k\mathbf{h}_j^H|^2, \frac{1}{M}|\mathbf{h}_k\mathbf{h}_l^H|^2\right) = \frac{1}{M^2}\mathbb{E}[|\mathbf{h}_k\mathbf{h}_k^H|^2] - 1$$

Let

$$X_k \triangleq \frac{1}{M}|\mathbf{h}_k\mathbf{h}_k^H|.$$

Since entries of $\mathbf{h}_k$ are i.i.d. following $\mathcal{CN}(0,1)$, X_k has the pdf of Gamma distribution $\phi(y; M, 1/M)$ and

$$\begin{aligned} \mathbb{E}[X_k^2] &= \mathbb{E}^2[X_k] + \mathrm{Var}[X] \\ &= 1 + \frac{1}{M} \end{aligned}$$

The covariance is thus

$$\mathrm{cov}\left(\frac{1}{M}|\mathbf{h}_k\mathbf{h}_j^H|^2, \frac{1}{M}|\mathbf{h}_k\mathbf{h}_l^H|^2\right) = \frac{1}{M}$$

For the denominator of ρ_{jl}, recall that $\frac{1}{M}|\mathbf{h}_k\mathbf{h}_j^H|^2$ is approximately distributed as $\phi(y;1,1)$. Then $\mathrm{Var}\left[\frac{1}{M}\left|\mathbf{h}_k\mathbf{h}_j^H\right|^2\right]$ equals to 1. From (2.6), the correlation coefficient is therefore given by

$$\rho_{jl} = \frac{1}{M}.$$

So $\frac{1}{M}\sum_{j=1,k\neq j}^{K}|\mathbf{h}_k\mathbf{h}_j^H|^2$ is a sum of $K-1$ correlated Gamma random variables with the same shape parameter of 1 and the same scale parameter of 1. And the correlation coefficient of any two of the Gamma variables is $1/M$. From Corollary 1 of [45], the pdf of $\frac{1}{M}\sum_{j=2}^{K}|\mathbf{h}_1\mathbf{h}_j^H|^2$ is

$$f_{Y_k}(y) = \prod_{i=1}^{K-1}\left(\frac{\sigma_1}{\sigma_i}\right)\sum_{j=0}^{\infty}\frac{\delta_j y^{K+j-2}e^{-y/\sigma_1}}{\sigma_1^{K+j-1}\Gamma(K+j-1)}, \tag{2.7}$$

where $\Gamma(\cdot)$ is the Gamma function. $\sigma_1 \leq \sigma_2 \leq \cdots \leq \sigma_{K-1}$ are the ordered eigenvalues of the $(K-1)\times(K-1)$ matrix $\mathbf{A}$, whose diagonal entries are 1 and off-diagonal entries are $1/\sqrt{M}$, and δ_j's are defined iteratively as

$$\begin{aligned}\delta_0 &= 1\\ \delta_{j+1} &= \frac{1}{j+1}\sum_{m=1}^{j+1}\left[\sum_{n=1}^{K-1}\left(1-\frac{\sigma_1}{\sigma_n}\right)^m\right]\delta_{j+1-m}.\end{aligned} \tag{2.8}$$

As $\mathbf{A}$ is a circulant matrix whose off-diagonal entries are the same, its eigenvalues can be calculated to be

$$\sigma_1 = \cdots = \sigma_{K-2} = 1-\frac{1}{\sqrt{M}},\ \ \sigma_{K-1} = 1+\frac{K-2}{\sqrt{M}}. \tag{2.9}$$

Then we have

$$f_{Y_k}(y) \approx \tilde{f}_{Y_k}(y) = \frac{\sigma_1}{\sigma_{K-1}}\sum_{j=0}^{\infty}\frac{\delta_j y^{K+j-2}e^{-y/\sigma_1}}{\sigma_1^{K+j-1}\Gamma(K+j-1)}, \tag{2.10}$$

Using (2.8) and (2.9), we have

$$\begin{aligned}
\delta_0 &= 1 \\
\delta_1 &= 1 - \frac{\sigma_1}{\sigma_{K-1}} \\
\delta_2 &= \left(1 - \frac{\sigma_1}{\sigma_{K-1}}\right)^2 \\
&\vdots \\
\delta_j &= \left(1 - \frac{\sigma_1}{\sigma_{K-1}}\right)^j
\end{aligned} \tag{2.11}$$

Substituting (2.9) and (2.11) into (2.10), we conclude the proof. □

Next, we discuss the properties of the pdf of the interference power. It can be seen from (2.5) that the interference power has a mixture distribution of infinite Gamma random variables with the same scale parameter $1 - 1/\sqrt{M}$ but different shape parameters. Also, the distribution is independent of the user index k.

The interference power pdf in (2.5) is in an infinite summation form. In reality, we can only evaluate it with finite terms. An approximation with the first L terms is as follows:

$$f_{Y_k,L}(y) = \frac{1-\eta}{1-\eta^L} \sum_{i=0}^{L-1} \eta^i \phi\left(y; K+i-1, 1-\frac{1}{\sqrt{M}}\right). \tag{2.12}$$

The coefficient $\left(1-\eta^L\right)^{-1}$ is to guarantee $\int_0^\infty f_{Y_k,L}\mathrm{d}y = 1$. When $L = 1$, we get

$$f_{Y_k,1}(y) = \phi\left(y; K-1, 1-\frac{1}{\sqrt{M}}\right). \tag{2.13}$$

This $L = 1$ approximation can also be obtained by assuming that the $K - 1$ terms in Y_k are independent to each other.

But notice that with the same scale parameter, Gamma distribution with a larger shape parameter has a larger tail. With the approximations in (2.12) and (2.13), the terms with the largest tails are ignored. They can cause loose approximation on the distribution tail. The loose tail in the pdf of the interference power also leads to the

inaccuracy of the derivation on outage probability. It is because that outage occurs when the interference power is large, so the SINR is less than the threshold. In another word, the outage probability behaviour is dominated by the tail part in the pdf of the interference power. In what follows, we derived an closed-form formula of the pdf, which gives accurate description on the pdf tail and then enables us to analyze the outage probability accurately.

Corollary 2.1. The pdf of Y_k can be rewritten into the following closed-form:

$$f_{Y_k}(y)=\frac{\sqrt{M}}{\sqrt{M}+K-2}\eta^{-(K-2)}\left[e^{-\frac{\sqrt{M}}{\sqrt{M}+K-2}y}-e^{-\frac{\sqrt{M}}{\sqrt{M}-1}y}\sum_{n=0}^{K-3}\left(\frac{\sqrt{M}}{\sqrt{M}-1}\eta\right)^n\frac{y^n}{n!}\right] \quad (2.14)$$

Proof. Notice that

$$\begin{aligned}&\sum_{i=0}^{\infty}\eta^i\phi\left(y;K+i-1,1-\frac{1}{\sqrt{M}}\right)\\&=\frac{\sqrt{M}}{\sqrt{M}-1}\eta^{-(K-2)}e^{-\frac{\sqrt{M}}{\sqrt{M}-1}y}\left(\sum_{n=0}^{\infty}-\sum_{n=0}^{K-3}\right)\left(\frac{\sqrt{M}}{\sqrt{M}-1}\eta\right)^n\frac{y^n}{n!}.\end{aligned}$$

It can be observed that

$$\sum_{n=0}^{\infty}\left(\frac{\sqrt{M}}{\sqrt{M}-1}\eta\right)^n\frac{y^n}{n!}$$

is the Taylor series for exponential function:

$$e^{\frac{\sqrt{M}\eta}{\sqrt{M}-1}y}=\sum_{n=0}^{\infty}\left(\frac{\sqrt{M}}{\sqrt{M}-1}\eta\right)^n\frac{y^n}{n!}.$$

Then we can obtain (2.14). □

From (2.14), it can be shown that for very large y, the first term becomes dominant since its exponent is large. However for general value of y and practical ranges of M and K (e.g., $M = 200$, $K = 10$), both terms have non-negligible contribution to the pdf. As K increases, the first term becomes more significant. As M increases, the first term is less significant. If only the limit case of $M\to\infty$ is considered, the effect of K will be eliminated from the pdf, leading to useless results.

Furthermore, the formula shows that the ratio of M and K does not dominate the interference behaviour. The complicated interaction of $\sqrt{M}$ and K is important for the performance.

2.4 Performance Analysis

In this section, we start with the outage probability analysis based on the pdf of the interference power Y_k (2.14). An analytical result of the outage probability of the massive MIMO system is derived. We then use the pdf of the interference power to derive the average sum-rate.

2.4.1 Outage Probability Analysis

From (2.3), the SINR of User k can be written as

$$\mathrm{SINR}_k = \frac{P_t M}{K} \cdot \frac{X_k^2}{(1 + \frac{P_t}{K} Y_k)}.$$

We first study the variances of X_k^2 and $1 + \frac{P_t}{K} Y_k$. The variance of X_k^2 can be expressed as

$$\mathrm{Var}(X_k^2) = \mathbb{E}[X_k^4] - \mathbb{E}^2[X_k^2]$$

Since X_k has the pdf of gamma distribution $\phi(y; M, 1/M)$, $\mathbb{E}[X_k^4]$ can be calculated by the moment generating function (MGF) $M_x(t)$ of gamma distribution, given by

$$M_x(t) = (1 - \alpha t)^{-\beta}$$

Recall that α and β are the shape parameter and the scale parameter of Gamma distribution. Then we have

$$\begin{aligned} \mathbb{E}[X_k^4] &= M_x^{(4)}(0) \\ &= \frac{1}{M^4}(M+3)(M+2)(M+1)M \end{aligned}$$

where $M_x^{(4)}(0)$ represents the fourth derivative of $M_x(t)$ at $t = 0$. Since $\mathbb{E}[X_k^2]$ can be achieved by

$$\begin{aligned}\mathbb{E}[X_k^2] &= \mathrm{Var}[X_k] + \mathbb{E}^2[X_k] \\ &= 1 + \frac{1}{M},\end{aligned}$$

the variance of X_k^2 is then

$$\begin{aligned}\mathrm{Var}[X_k^2] &= \frac{4}{M} + \frac{10}{M^2} + \frac{6}{M^3} \\ &= \frac{4}{M} + o\left(\frac{1}{M}\right).\end{aligned} \tag{2.15}$$

$o(\cdot)$ is the Landau symbol. Define

$$f(M) = \frac{10}{M^2} + \frac{6}{M^3},$$

and

$$g(M) = \frac{1}{M}.$$

Then $f(M) = o\left(g(M)\right)$ represents that $f(M)$ has a higher order of smallness with respect to $g(M)$ as M converges to infinity, defined as

$$\lim_{M\to\infty} \frac{f(M)}{g(M)} = 0$$

So the first term $4/M$ in (2.15) becomes dominant when M is large.

The variance of the interference power is expressed as

$$\mathrm{Var}(Y_k) = \mathbb{E}[Y_k^2] - \mathbb{E}^2[Y_k].$$

By (2.10), the mean of Y_k is given by

$$\mathbb{E}[Y_k] = \int_0^\infty y \cdot \frac{\sigma_1}{\sigma_{K-1}} \sum_{j=0}^{\infty} \frac{\delta_j y^{K+j-2} e^{-y/\sigma_1}}{\sigma_1^{K+j-1}\Gamma(K+j-1)} \mathrm{d}y$$

$$= \frac{\sigma_1^2}{\sigma_{K-1}} \sum_{j=0}^{\infty} \left(1 - \frac{\sigma_1}{\sigma_{K-1}}\right)^j (K + j - 1)$$

To calculate the summation term

$$S = \sum_{j=0}^{\infty} \left(1 - \frac{\sigma_1}{\sigma_{K-1}}\right)^j (K + j - 1),$$

we expand the summation as

$$\begin{aligned} S = (K-1) + \left(1 - \frac{\sigma_1}{\sigma_{K-1}}\right) K + \left(1 - \frac{\sigma_1}{\sigma_{K-1}}\right)^2 (K+1) + \cdots \\ + \left(1 - \frac{\sigma_1}{\sigma_{K-1}}\right)^n (K + n - 1) + \cdots \end{aligned}$$

Multiplying $\left(1 - \frac{\sigma_1}{\sigma_{K-1}}\right)$ on both side of the equation, we have

$$\begin{aligned} \left(1 - \tfrac{\sigma_1}{\sigma_{K-1}}\right) S = \left(1 - \frac{\sigma_1}{\sigma_{K-1}}\right) (K-1) + \left(1 - \frac{\sigma_1}{\sigma_{K-1}}\right)^2 K \\ + \cdots + \left(1 - \frac{\sigma_1}{\sigma_{K-1}}\right)^n (K + n - 2) + \cdots \end{aligned}$$

Then $S - \left(1 - \frac{\sigma_1}{\sigma_{K-1}}\right) S$ is

$$\frac{\sigma_1}{\sigma_{K-1}} S = (K-1) + \sum_{i=1}^{\infty} \left(1 - \frac{\sigma_1}{\sigma_{K-1}}\right)^i$$

and

$$\begin{aligned} \mathbb{E}[Y_k] &= \frac{\sigma_1^2}{\sigma_{K-1}} S \\ &= (K-2)\sigma_1 + \sigma_{K-1} \\ &= K - 1 \end{aligned} \tag{2.16}$$

Next, we calculate the variance of Y_k^2. It can be shown that

$$\mathbb{E}[Y_k^2] = \frac{\sigma_1}{\sigma_{K-1}} \sum_{j=0}^{\infty} \delta_j \frac{\sigma_1^2}{\Gamma(K + j - 1)} \int_0^{\infty} y^{K+j} e^{-y} \mathrm{d}y$$

$$= \frac{\sigma_1^3}{\sigma_{K-1}} \sum_{j=0}^{\infty} \left(1 - \frac{\sigma_1}{\sigma_{K-1}}\right)^j \left((K+j-1) + (K+j-1)^2\right)$$

The first term has been solved as above. For the second term

$$T_1 = \sum_{j=0}^{\infty} \left(1 - \frac{\sigma_1}{\sigma_{K-1}}\right)^j (K+j-1)^2,$$

we follow the similar method and achieve that

$$\frac{\sigma_1}{\sigma_{K-1}} T_1 = (K-1)^2 + \sum_{n=1}^{\infty} \left(1 - \frac{\sigma_1}{\sigma_{K-1}}\right)^n (2K+2n-3). \tag{2.17}$$

Then for the summation

$$T_2 = \sum_{n=1}^{\infty} \left(1 - \frac{\sigma_1}{\sigma_{K-1}}\right)^n (2K+2n-3),$$

we have

$$\frac{\sigma_1}{\sigma_{K-1}} T_2 = \left(1 - \frac{\sigma_1}{\sigma_{K-1}}\right)(2K-1) + 2\frac{\sigma_{K-1}}{\sigma_1} \left(1 - \frac{\sigma_1}{\sigma_{K-1}}\right)^2. \tag{2.18}$$

Substituting (2.17) and (2.18) into (2.16), the variance of Y_k is given by

$$\begin{aligned} \mathrm{Var}[Y_k] &= (K-2)\sigma_1^2 + \sigma_{K-1}^2 \\ &= K - 1 + (K-1)(K-2)/M. \end{aligned} \tag{2.19}$$

Thus, the variance of $1 + \frac{P_t}{K} Y_k$ is given by

$$\mathrm{Var}\left(1 + \frac{P_t}{K} Y_k\right) = \frac{P_t^2 (K-1)}{K^2} \left(1 + \frac{K-2}{M}\right) > \frac{P_t^2 (K-1)}{K^2}.$$

When $M \to \infty$, it can be shown in (2.15) that the variance of the desired signal power X_k^2 decreases to 0, meaning that the signal power becomes deterministic. However, this is not the case for the interference power, whose variance is not negligible for reasonable K and P_t. When M is large, the variance of the interference

power is significantly larger than the variance of the signal power when

$$\frac{P_t^2(K-1)}{K^2} \gg \frac{1}{M}$$

which can be approximated as $P_t^2 M \gg K$. Thus for tractable analysis, we treat X_k^2 as deterministic and approximate it by its average. This is the same as using asymptotic deterministic equivalence method for $M \to \infty$. But different to existing work, we keep Y_k as a random variable in the outage probability analysis below.

Let γ_{th} be the SINR threshold. Define that outage occurs when the SINR is less than the threshold. The outage probability of User k can thus be approximated as follows.

$$\begin{aligned} P_{\text{out}} &= \mathbb{P}\left(P_u M \frac{X_k^2}{1+\frac{P_t}{K}Y_k} < \gamma_{th} \right) \\ &\approx \mathbb{P}\left(\frac{P_t}{K} M \frac{1+\frac{1}{M}}{1+\frac{P_t}{K}Y_k} < \gamma_{th} \right) \\ &= \begin{cases} 1 & \text{if } \gamma_{th} \geq M\frac{P_t}{K} \\ \mathbb{P}\left(Y_k > \frac{M+1}{\gamma_{th}} - \frac{K}{P_t} \right) & \text{otherwise} \end{cases}. \end{aligned}$$

When $\gamma_{th} \leq MP_u$, from (2.14), we have the outage probability results as shown in (2.20), where $\Gamma(s,x) \triangleq \int_x^\infty t^{s-1}e^{-t}\mathrm{d}t$ is the upper incomplete gamma function.

$$\begin{aligned} P_{out} \approx\ & \frac{\sqrt{M}}{\sqrt{M}+K-2}\eta^{-(K-2)} \left[\int_{\frac{M+1}{\gamma_{th}}-\frac{K}{P_t}}^{\infty} e^{\frac{-\sqrt{M}}{\sqrt{M}+K-2}y} dy \right. \\ & \left. - \sum_{n=0}^{K-3} \eta^n \left(\frac{\sqrt{M}}{\sqrt{M}-1} \right)^n \int_{\frac{M+1}{\gamma_{th}}-\frac{K}{P_t}}^{\infty} \frac{y^n}{n!} e^{-\frac{\sqrt{M}}{\sqrt{M}-1}y} \mathrm{d}y \right] \\ =\ & \eta^{-(K-2)} e^{-\frac{\sqrt{M}}{\sqrt{M}+K-2}\left(\frac{M+1}{\gamma_{th}}-\frac{K}{P_t}\right)} \\ & - (1-\eta) \sum_{n=0}^{K-3} \frac{1}{n!} \eta^{n-K+2} \Gamma\left(n+1, \frac{\sqrt{M}}{\sqrt{M}-1}\left(\frac{M+1}{\gamma_{th}} - \frac{K}{P_t} \right) \right). \end{aligned} \quad (2.20)$$

(2.20) shows that the outage probability does not converge to 0 even if the total transmit power goes large. This is due to the MRT precoding which cannot fully eliminate the user-interference. When M goes to infinity, it is possible to simplify

(2.20) using the asymptotic behavior of incomplete gamma function. With this asymptotic approximation, the first term becomes dominant as $M \to \infty$. However, as the approximation needs very large M (e.g., several thousands) to be tight, the simplification is not appropriate for practical scenarios. The result in (2.20) can help the design of massive MIMO systems for the desired outage level. For example, we can decide how many users can be served simultaneously by the massive BS for a given γ_{th} value.

From the derivations given above, it is seen that the outage probability can be derived and analyzed since the random property of SINR is investigated and the pdf of the interference power is derived. In existing work, since the random property of SINR was not considered and only the asymptotic deterministic equivalence of the SINR was derived, the outage probability cannot be obtained.

2.4.2 Sum-Rate Analysis

Recall that the SINR at User k is given by

$$\mathrm{SINR}_k = \frac{P_t M}{K} \cdot \frac{X_k^2}{1 + \frac{P_t}{K} Y_k}.$$

Then we have the achievable rate written as

$$R_k = \log_2 \left(1 + \frac{P_t M}{K} \cdot \frac{X_k^2}{1 + \frac{P_t}{K} Y_k} \right).$$

As discussed above, the variations of the signal power random variable X_k^2 is relatively little to that of the interference power Y_k. So for the derivation of the sum-rate, we still replace X_k^2 with its average and only keep Y_k random. In this case, the average achievable rate can be given by

$$\begin{aligned} \mathbb{E}[R_k] &= \mathbb{E}\left[\log_2 \left(1 + \frac{P_t}{K} M \cdot \frac{1 + \frac{1}{M}}{1 + \frac{P_t}{K} Y_k} \right) \right] \\ &= \log_2 \left(1 + \frac{P_t}{K} M \right) + \mathbb{E}\left[\log_2 \left(1 + \frac{P_t}{K + P_t M} Y_k \right) \right] \end{aligned}$$

$$-\mathbb{E}\left[\log_2\left(1+\frac{P_t}{K}Y_k\right)\right]. \tag{2.21}$$

Since the pdf of Y_k is provided in Section 2.3, the average achievable rate can be derived by integral calculations with the following integral formula [46]

$$\int_0^\infty \log_2(1+rx)x^b e^{-\frac{x}{2a}}\mathrm{d}x = \frac{(2a)^{b+1}}{\ln 2}b!e^{\frac{1}{2ra}}\sum_{i=0}^{b}E_{i+1}\left(\frac{1}{2ra}\right), \tag{2.22}$$

where $E_n(x)$ is the exponential integral, given by

$$E_n(x) = \int_1^\infty \frac{e^{-xt}}{t^n}\mathrm{d}t.$$

The average achievable rate can be calculated to be

$$\begin{aligned}\mathbb{E}[R_k]=&\log_2\left(1+\frac{P_t}{K}M\right)+\frac{\eta^{-(K-2)}}{\ln 2}e^{\frac{\sqrt{M}K}{(\sqrt{M}+K-2)P_t}}\left[e^{\frac{\sqrt{M}MP_t}{(\sqrt{M}+K-2)P_t}}E_1\left(\frac{\sqrt{M}(P_tM+K)}{(\sqrt{M}+K-2)P_t}\right)\right.\\&\left.-E_1\left(\frac{K\sqrt{M}}{(\sqrt{M}+K-2)P_t}\right)\right]-\frac{1-\eta}{\ln 2}\eta^{-(K-2)}e^{\frac{K\sqrt{M}}{(\sqrt{M}-1)P_t}}\left[e^{\frac{\sqrt{M}MP_t}{(\sqrt{M}-1)P_t}}\sum_{n=0}^{K-3}\eta^n\right.\\&\left.\cdot\sum_{i=0}^{n}E_{i+1}\left(\frac{\sqrt{M}(K+P_tM)}{(\sqrt{M}-1)P_t}\right)-\sum_{n=0}^{K-3}\eta^n\sum_{i=0}^{n}E_{i+1}\left(\frac{K\sqrt{M}}{(\sqrt{M}-1)P_t}\right)\right]\end{aligned} \tag{2.23}$$

and the average sum-rate is

$$R_{\text{sum}} = K\cdot\mathbb{E}[R_k].$$

When $M\to\infty$, the interference power converges to its average by the law of large numbers. Then the asymptotic deterministic equivalence of the SINR can be shown as

$$\text{SINR}_{k,asym} = \frac{M}{K}\frac{P_t(1+\frac{1}{M})}{1+P_t\frac{K-1}{K}}. \tag{2.24}$$

When $K, M\to\infty$ but with fixed ratio, we have

$$\text{SINR}_{k,asym}\to\frac{M}{K}\frac{P_t}{1+P_t}, \tag{2.25}$$

which is the same as the SINR result derived in [12]. The asymptotic sum-rate is given by

$$R_{\text{asym}} = K \log_2(1 + \text{SINR}_{k,asym}). \tag{2.26}$$

Although (2.23) is complicate, it has a better match to the Monte-Carlo simulation than the asymptotic result of sum-rate in [12]. Moreover, the result in (2.24) has a tighter match to the Monte-Carlo simulation of SINR than (2.25), especially for small K and finite M.

When a user is in outage, its communication is unsuccessful. To measure the system performance of effective communications, outage capacity is defined to calculate the sum of the achievable rates for the users not in outage. With the results of the outage probability and the sum-rate, the analytical outage capacity can be written as

$$R_{\text{out}} = (1 - P_{\text{out}}) \cdot R_{\text{sum}} \tag{2.27}$$

2.5 Simulation Results

In this section, we provide simulation results to verify the accuracy of the approximate pdf of the interference power. Besides, we draw the figures for the results of outage probability and the sum-rate.

In Fig. 2.2, for a system with $M = 100$ and $K = 10, 30$, the simulated pdf (via Monte-Carlo simulation) of the interference power is shown. We compare the Monte-Carlo simulations with the approximate pdf in (2.12) for $L = 10$, the approximation in (2.13), and the closed-form pdf in (2.14). This figure shows that (2.14) matches tightly with the simulation for all y range and both K values. Since the $L = 1$ approximation in (2.13) only keep the first term in an infinite summation series and ignore a number of large tail terms, it has significant offset to the left which leads to a much loose tail compared to the Monte-Carlo simulation. The $L = 10$ approximation has a better match than (2.13) at $K = 10$ and it is close to the result in (2.14). But for $K = 30$, it also has noticeable offset and underestimates

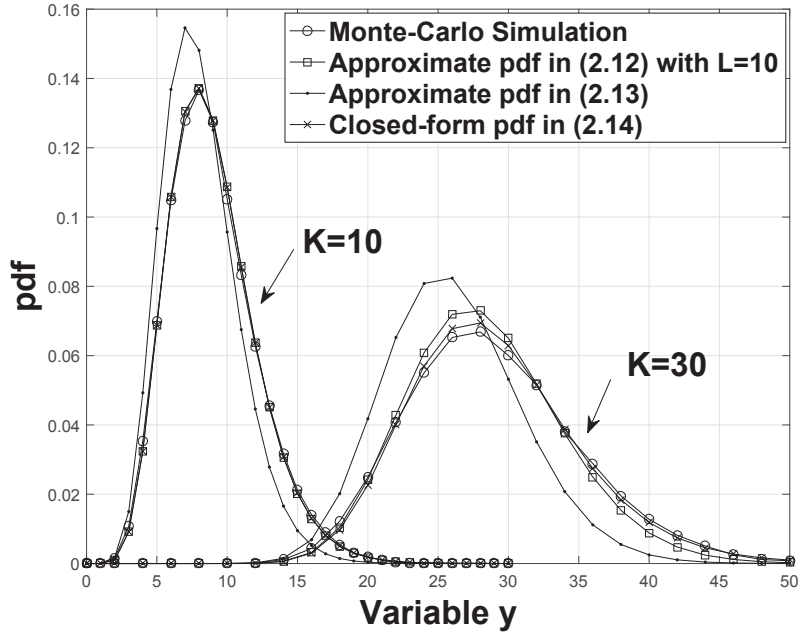

Fig. 2.2. Comparison of the pdfs of the term $\frac{1}{M}\sum_{j=1,k\neq j}^{K}|\mathbf{h}_k\mathbf{h}_j^H|^2$ for $M = 100$ and $K = 10, 30$.

the tail of the distribution as we have discussed in Section 2.3.

Fig. 2.3 shows the outage probability for different number of users. Our analytical result in (2.20) has a tight match to the Monte-Carlo simulation for all range of K. When $M = 100$, $P_t = 10$dB, $\gamma_{th} = 10$dB, the outage probability is more than 10% when there are 7 users or more. When the number of antennas increases from 100 to 200, the outage probability for 7 users is below 0.1%. So massive MIMO can improve the performance of outage probability due to the large number of antennas. Fig. 2.4 shows the outage probability for different number of antennas. The BS serves 10 users simultaneously and the outage threshold is 10dB. It can be seen that the analytical result is accurate even for small M. When P_t is 20dB, 130 antennas are needed to achieve 10% outage probability. When P_t decrease to 10dB, only 10 more antennas are required to keep the same outage probability. It is shown that the outage probability of massive MIMO does not have a considerable difference with the change of the transmit power in massive MIMO. Fig. 2.5 shows the outage probability for different transmit power. The number of users is 10 and the

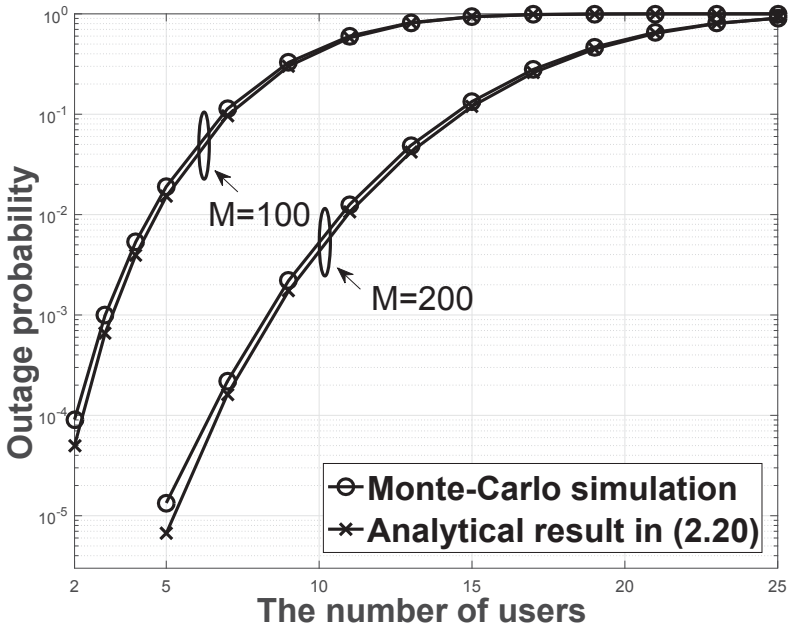

Fig. 2.3. Outage probability v.s. K. $P_t = 10$dB. $\gamma_{th} = 10$dB.

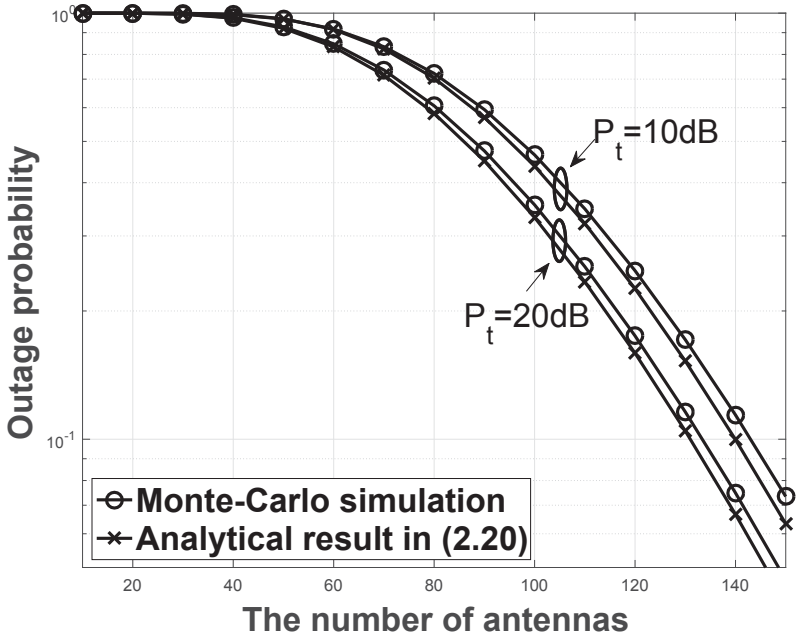

Fig. 2.4. Outage probability v.s. M. $K = 10$, $\gamma_{th} = 10$dB.

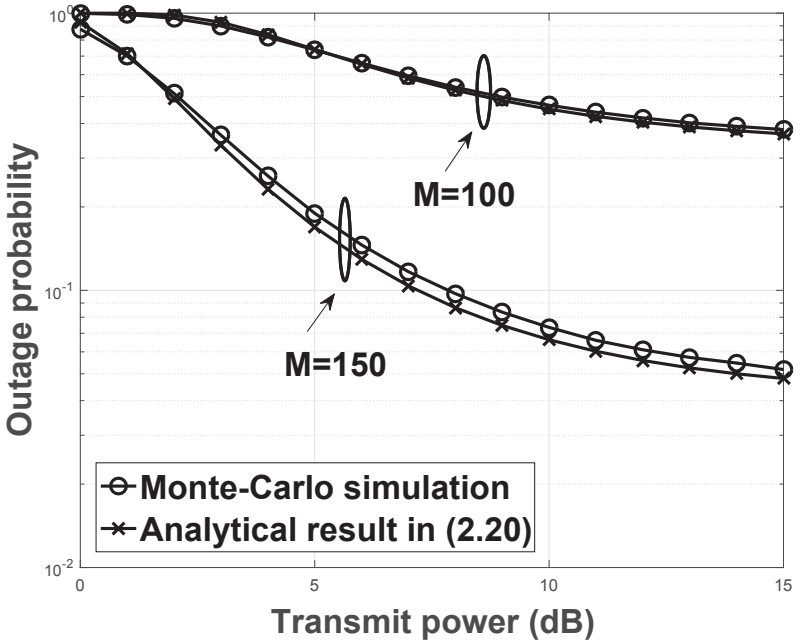

Fig. 2.5. Outage probability v.s. P_t. $K = 10, \gamma_{th} = 10$dB.

outage threshold is 10dB. Even when P_t increases, the outage probability does not decrease to zero. This is due to the MRT precoding which can not fully eliminates the use-interference. When the number of antennas is 100, the outage probability is above 0.3 for $P_t = 15$dB. As the number of antennas increases to 150, the outage probability is below 0.1 for $P_t = 7$dB. It is clearly shown that the large number of antennas can improve the outage performance more significantly than the high transmit power .

Fig. 2.6 shows the sum-rate for different number of users ranging from 5 to 40. The number of antennas is 100 and the total power transmit is 10dB. As the number of users increases, the sum-rate has a nearly linear increase. Also, our analytical result (2.23) tightly match the Monte-Carlo simulations for all range of K while the asymptotic result in [12] has a noticeable gap from the Monte-Carlo simulation. Fig. 2.7 shows the sum-rate for different number of antennas ranging from 50 to 200. The number of users is 10 and the total transmit power is 10dB. When the number of antennas increases, the sum-rate increases. It is also shown that our analytical result (2.23) is more accurate than the asymptotic result in [12].

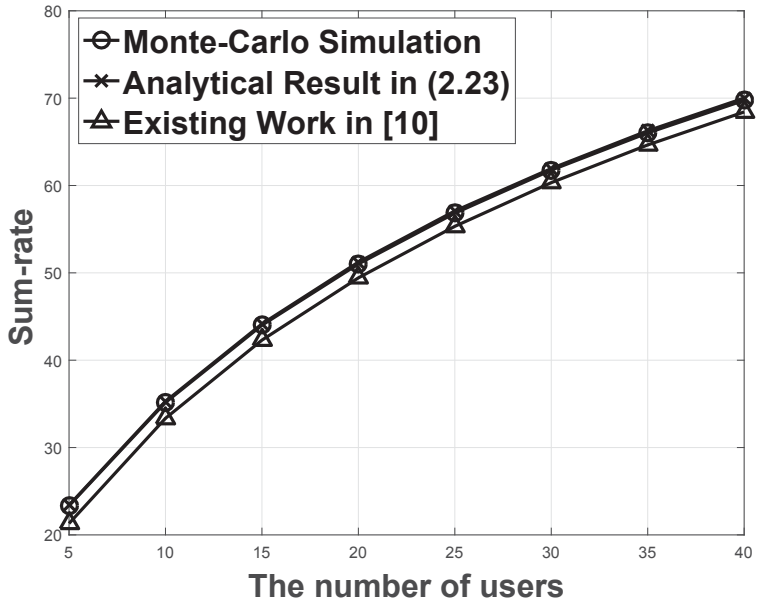

Fig. 2.6. Sum-rate vs. the number of users K. $M = 100$, $P_t = 10$dB.

Fig. 2.8 depicts the sum-rate for different total transmit power P_t ranging from 5dB to $15dB$. It can be clearly observed that as P_t increases, the sum-rate increases with a slow rate. Fig. 2.9 shows the outage capacity for different number of users. The number of antennas is 100 and the total transmit power is 10dB. When $\gamma_{th} = 7$dB, the outage capacity overlaps with the curve with $\gamma_{th} = 5$dB for the small number of users. However, when the number of users is larger than 10, outage occurs among the users and the outage capacity increases at a decreasing rate. When the number of users reaches 15, the outage capacity starts decreasing. When the number of users grows to 35, the outage capacity decreases to 0 and all the users are at outage. The figure shows the importance of outage probability analysis. As K increases, even though the theoretical sum-rate increases, more users can be in outage and the actual system throughput can be low.

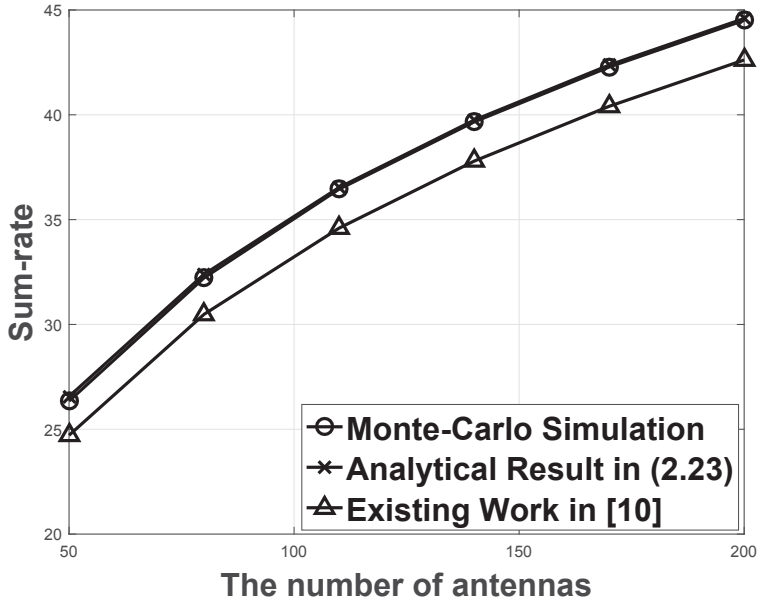

Fig. 2.7. Sum-rate vs. the number of antennas M. $K = 10$, $P_t = 10$dB.

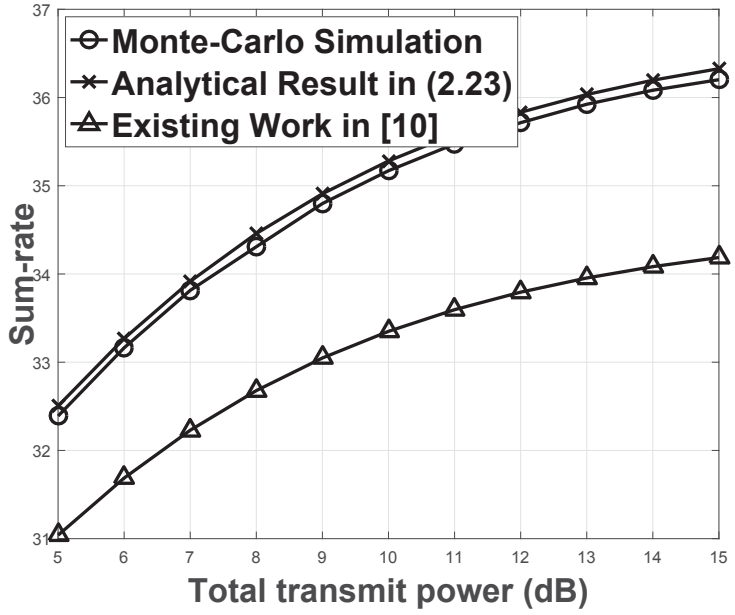

Fig. 2.8. Sum-rate vs. the total transmit power P_t. $K = 10$, $M = 100$.

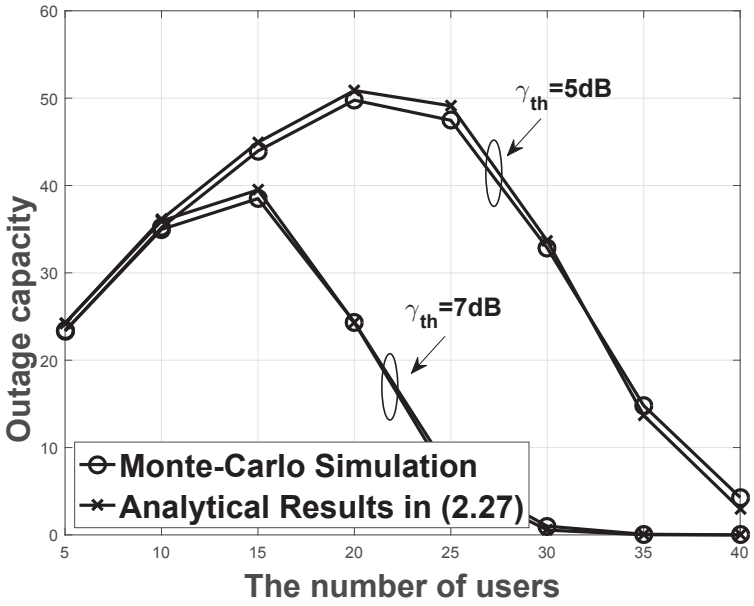

Fig. 2.9. Outage capacity vs. K. $M = 100$, $P_t = 10$dB.

2.6 Conclusion

In Chapter 2, a single-cell multiuser massive MIMO is investigated under MRT precoding. The number of antennas is assume to be large but finite, and the number of users is assumed to be moderate. We analyze the random property of the interference power with large-scale antenna array by central limit theory. The approximate pdf of the interference power is derived. By comparing between the variances of the signal power and the interference plus the noise power, we treat the interference power as random and replace the signal power random variable with its average. The analytical results of the outage probability and the average sum-rate in massive MIMO are derived. The simulation results show that the system sum-rate increases with the growing number of users while outage probability and outage capacity are poor when there are too many users.

Chapter 3

Modified MRT Precoding Under Per-Antenna Power Constraint in Massive MIMO and Performance Analysis

In this chapter, we consider per-antenna power constraint in a single-cell multi-user massive MIMO system. A modified MRT precoding is proposed to meet the power constraint at each antenna. Rayleigh flat fading channel model is used and perfect CSI at the BS is assumed. The analysis of the outage probability and the sum-rate is provided after deriving the distribution of the interference power. Simulation results show that the proposed modified MRT precoding can improve the performance of massive MIMO even with a strict power constraint.

3.1 Background and Related Work

Antenna transmit power is an important factor for massive MIMO transceiver designs. For the system downlink, while several precoding schemes have been widely used, such as MRT, ZF, and WF precoding, they consider a total transmit power constraint. However, in practical systems, each antenna at the BS is equipped with

an individual power amplifier (PA). To obtain linear power amplification without distortion, a PA needs to operate within its effective output power interval. When high power output is required which is beyond a PA's effective operation interval, non-linear distortion can occur to the signal. To avoid the distortion, each antenna needs to have its own power constraint depending on its own PA. Thus, it is more practical to consider the per-antenna power constraint than the total transmit power constraint in the precoding design.

There have been some papers [47]–[49] for MU-MIMO systems or multi-user massive MIMO systems with per-antenna power constraint. In [47], for single-cell MU-MIMO downlink with perfect CSI, two optimal precoding schemes are provided under per-antenna transmit power constraint. One scheme is to minimize the per-antenna transmit power, and the other scheme is to achieve the channel capacity. The downlink optimization problems are solved by transforming them into a dual uplink problem with an uncertain noise. In [48], single-cell MU-MIMO downlink with perfect CSI is considered. An optimum ZF precoding is designed by maximizing the minimum rate in the system under per-antenna power constraint. It is shown that conventional ZF precoding is suboptimal when per-antenna power constraint is considered and the proposed optimum ZF precoding greatly increase the achievable rate when the number of BS antennas is large. In [49], a multi-user massive MIMO downlink with frequency-selective channel is considered. It is assumed that the BS has the knowledge of downlink CSI. A low complexity precoding is proposed by which the per-antenna transmit signals has constant-envelop (CE). The proposed precoding is achieved by minimizing the inter-user interference under the constraint of the per-antenna transmit signal envelop. The optimization problem is solved by a low complexity iterative algorithm. The per-antenna CE constraint is more strict than the one in [47], [48]. It is shown that for a fixed desired sum-rate, the required total transmit power for the proposed per-antenna CE precoding is less than the precoding schemes with total transmit power constraint.

3.2 System Model and Modified MRT Precoding

To clearly explain the new precoding scheme, we rewrite the downlink channel matrix as

$$\mathbf{H} = \begin{bmatrix} \mathbf{h}_1 & \mathbf{h}_2 & \cdots & \mathbf{h}_M \end{bmatrix},$$

where $\mathbf{h}_j$ (the jth column of $\mathbf{H}$) is the $K \times 1$ channel vector from the jth BS antenna to K users. Let

$$\mathbf{q} = \begin{bmatrix} q_1 \\ q_2 \\ \vdots \\ q_K \end{bmatrix}$$

be the $K \times 1$ symbol vector intended for K users. All entries of $\mathbf{q}$ are independent of each other. The power of each data symbol is normalized to 1, i.e., $\mathbb{E}[|q_k|^2] = 1$. In the downlink, the BS first precodes the $K \times 1$ information vector into an $M \times 1$ coded vector $\mathbf{s}$ via an $M \times K$ precoding matrix $\mathbf{W}$ as follows:

$$\mathbf{s} = \alpha \mathbf{W} \mathbf{q} = \alpha \begin{bmatrix} \mathbf{w}_1 \mathbf{q} \\ \mathbf{w}_2 \mathbf{q} \\ \vdots \\ \mathbf{w}_M \mathbf{q} \end{bmatrix}, \tag{3.1}$$

α is a coefficient used for power scaling and $\mathbf{w}_j$ is the jth row of $\mathbf{W}$.

As mentioned in Chapter 1, MRT, ZF, and MMSE precoding schemes are used widely in massive MIMO. Especially, MRT precoding has attracted a lot of interests due to its desirable balance between computational complexity and performance in massive MIMO [37]. In MRT precoding, with the average total power constraint P_t, we have

$$\alpha_{\mathrm{MRT}} = \sqrt{\frac{P_t}{KM}} \quad \text{and} \quad \mathbf{W}_{\mathrm{MRT}} = \mathbf{H}^H. \tag{3.2}$$

In real systems, each antenna is equipped with an individual PA which limits the operation region of the power for the corresponding antenna. Thus per-antenna power constraint is more practical in the study of massive MIMO donwlink than total power constraint. From (3.1), the transmit power at the jth antenna (averaged over the symbol vector $\mathbf{q}$) can be calculated as

$$\mathbb{E}\left[|\alpha \mathbf{w}_j \mathbf{q}|^2\right] = \alpha^2 |\mathbf{w}_j|^2.$$

Then for MRT precoding, the transmit power of the jth antenna is $\frac{P_t}{KM}|\mathbf{h}_j|^2$. So the transmit power of each antenna varies with different channel realizations. And for a given general channel realization, the transmit powers at different BS antennas are different. Thus standard MRT precoding does not apply for massive MIMO systems under per-antenna power constraint.

We consider the precoding design for massive MIMO systems with per-antenna power constraint P_a. For the optimal precoding design, one method is to formulate an optimization problem with respect to the precoding matrix and search for numerical solutions via optimization theory. However, such solutions usually have high computational complexity and performance analysis is not available. Instead, we modify the standard MRT precoding to incorporate the per-antenna power constraint. The proposed precoding matrix is as follows:

$$\mathbf{W} = \begin{bmatrix} \frac{\sqrt{K}}{||\mathbf{h}_1||}\mathbf{h}_1^H \\ \\ \frac{\sqrt{K}}{||\mathbf{h}_2||}\mathbf{h}_2^H \\ \\ \vdots \\ \\ \frac{\sqrt{K}}{||\mathbf{h}_M||}\mathbf{h}_M^H \end{bmatrix}.$$

First, with this design, the transmit power of the ith BS antennas (averaged over

$\mathbf{q}$) can be calculated by

$$\begin{aligned}\alpha^2|\mathbf{w}_i|^2 &= \frac{P_a}{K} \cdot \frac{K||\mathbf{h}_i||^2}{||\mathbf{h}_i||^2} \\ &= P_a,\end{aligned}$$

which is independent of the channel realization and is the same for all BS antennas. Since the transmit power of each antenna is fixed as P_a, the total transmit power is fixed as MP_a. Define the total transmit power by P_t, then we have

$$P_t = MP_a.$$

Second, compared to standard MRT precoding in (3.2), we have

$$\mathbf{W} = \mathbf{D}\mathbf{W}_{\text{MRT}}, \tag{3.3}$$

where $\mathbf{D} = \text{diag}\Big(\frac{\sqrt{K}}{||\mathbf{h}_1||}, \frac{\sqrt{K}}{||\mathbf{h}_2||}, \cdots, \frac{\sqrt{K}}{||\mathbf{h}_M||}\Big)$. Thus, the modified MRT precoding can be seen as the combination of the MRT precoding and a diagonal antenna power scaling matrix. The proposed modified MRT precoding still holds the idea of the standard MRT percoding scheme to maximize the desired signal power. Also, the proposed low-complexity precoding design is in closed-form and allows theoretical performance analysis.

To the best of our knowledge, in the literature, only column-normalization has been used on the MRT precoding matrix [50], [51]. Compared to our proposed precoding scheme in (3.3), the column-normalized MRT precoding is the same as right multiplying $\mathbf{W}_{\text{MRT}}$ by a $K \times K$ diagonal matrix. But under this precoding, the transmit power for each antenna still varies with the channel realization. Thus it does not guarantee per-antenna power constraint. Recall that Rayleigh fading channel is assumed, as M goes to infinity, the norm of each column-vector of $\mathbf{H}^H$ divided by M converges to 1. Thus, the column-normalization scheme reduces to the standard MRT precoding.

With (3.3), the received signal vector $\mathbf{x}$ with the modified MRT precoding can

be written as

$$\mathbf{x} = \sqrt{\frac{P_a}{K}}\mathbf{H}\mathbf{D}\mathbf{H}^H\mathbf{q} + \mathbf{n}, \tag{3.4}$$

where $\mathbf{n}$ is the noise vector whose entries are distributed as i.i.d. $\mathcal{CN}(0,1)$. It can be shown that the channel gains are added coherently for the diagonal entries of $\mathbf{H}\mathbf{D}\mathbf{H}^H$, similar to $\mathbf{H}\mathbf{H}^H$ in the standard MRT precoding scheme but with different power scaling. The received signal at User k with the modified MRT precoding is

$$\begin{aligned} x_k = &\sqrt{\frac{P_a}{K}}\sum_{j=1}^{M}\frac{\sqrt{K}}{||\mathbf{h}_j||}|h_{kj}|^2 q_k \\ &+\sqrt{\frac{P_a}{K}}\sum_{i=1,i\neq k}^{K}\sum_{j=1}^{M}\frac{\sqrt{K}}{||\mathbf{h}_j||}h_{kj}\overline{h}_{ij}q_i + n_k, \end{aligned} \tag{3.5}$$

where h_{kj} is the kth element of $\mathbf{h}_j$ and $\overline{h}_{ij}$ is the complex conjugate of h_{ij}. n_k is the kth entry of $\mathbf{n}$. From (3.5), the received SINR at User k can be calculated to be

$$\begin{aligned} \mathrm{SINR}_k &= \frac{\frac{P_a}{K}\left|\sum_{j=1}^{M}\frac{\sqrt{K}}{||\mathbf{h}_j||}|h_{kj}|^2 q_k\right|^2}{\mathrm{Var}[n_k] + \frac{P_a}{K}\left|\sum_{i=1,i\neq k}^{K}\sum_{j=1}^{M}\frac{\sqrt{K}}{||\mathbf{h}_j||}h_{kj}\overline{h}_{ij}q_i\right|^2} \\ &= \frac{P_a M^2}{K}\frac{\left|\frac{1}{M}\sum_{j=1}^{M}\frac{\sqrt{K}}{||\mathbf{h}_j||}|h_{kj}|^2 q_k\right|^2}{1 + \frac{P_a M}{K}\left|\sum_{i=1,i\neq k}^{K}\sum_{j=1}^{M}\frac{1}{M}\frac{\sqrt{K}}{||\mathbf{h}_j||}h_{kj}\overline{h}_{ij}q_i\right|^2}, \end{aligned}$$

Since $\{q_k\}_{k=1}^K$ is distributed as i.i.d. $\mathcal{CN}(0,1)$, the received SINR at User k averaged over $\{q_k\}_{k=1}^K$ can be derived as

$$\mathrm{SINR}_k = \frac{P_a M^2}{K}\frac{\left|\frac{1}{M}\sum_{j=1}^{M}\frac{\sqrt{K}}{||\mathbf{h}_j||}|h_{kj}|^2\right|^2}{1 + \frac{P_a M}{K}\sum_{i=1,i\neq k}^{K}\frac{1}{M}\left|\sum_{j=1}^{M}\frac{\sqrt{K}}{||\mathbf{h}_j||}h_{kj}\overline{h}_{ij}\right|^2},$$

Denote

$$X_k \triangleq \frac{1}{M}\sum_{j=1}^{M}\frac{\sqrt{K}}{||\mathbf{h}_j||}|h_{kj}|^2. \tag{3.6}$$

Then X_k^2 is the received signal power component. Also denote

$$Y_k \triangleq \sum_{i=1, i\neq k}^{K} \frac{1}{M} \left| \sum_{j=1}^{M} \frac{\sqrt{K}}{||\mathbf{h}_j||} h_{kj} \overline{h}_{ij} \right|^2, \tag{3.7}$$

which is the interference power experienced by User k. Then the SINR at User k can be written as

$$\mathrm{SINR}_k = \frac{P_a M^2}{K} \frac{X_k^2}{1 + \frac{P_a M}{K} Y_k}. \tag{3.8}$$

3.3 Analysis on Signal and Interference Power

Recall that the desired signal component for User k is X_k, which is defined in (3.6). The following lemma is proved to help the analysis on X_k.

Lemma 3.1. Define

$$Z \triangleq \sqrt{M} \left(X_k - \sqrt{K} \frac{(K - \frac{1}{2})!}{K!} \right).$$

When $M \to \infty$, Z converges in distribution to a real Gaussian random variable whose mean is zero and whose variance is $\frac{2K}{K+1} - K \left(\frac{(K-\frac{1}{2})!}{K!} \right)^2$, i.e.,

$$Z \xrightarrow{d} \mathcal{N} \left(0, \frac{2K}{K+1} - K \left[\frac{(K - \frac{1}{2})!}{K!} \right]^2 \right). \tag{3.9}$$

Proof. To approximate the distribution of X_k by central limit theory, we need find the mean and the variance of $\frac{|h_{kj}|^2}{|\mathbf{h}_j|}$.

Denote $A_{kj} \triangleq |h_{kj}|^2$. Since h_{kj} is distributed as $\mathcal{CN}(0, 1)$, A_{kj} has an exponential distribution with the rate parameter of 1. Denote

$$B_{kj} \triangleq \sum_{i=1, i\neq k}^{K} |h_{ij}|^2.$$

Since B_{kj} is the sum of $K - 1$ exponential random variables with same rate param-

eter of 1, it is distributed as $\mathrm{Erlang}(K-1,1)$ where

$$\mathrm{Erlang}(s,t) = \frac{t^s}{(s-1)!}x^{s-1}e^{-tx}.$$

The mean of $\frac{|h_{kj}|^2}{||\mathbf{h}_j||}$ is given by

$$\begin{aligned}\mathbb{E}\left[\frac{|h_{kj}|^2}{||\mathbf{h}_j||}\right] &= \mathbb{E}\left[\frac{A_{kj}}{\sqrt{A_{kj}+B_{kj}}}\right] \\ &= \frac{2}{(K-2)!}\int_0^\infty x^{K-2}\int_{\sqrt{x}}^\infty (y^2-x)e^{-y^2}\mathrm{d}y\mathrm{d}x\end{aligned}$$

Define

$$I = \int_{\sqrt{x}}^\infty y^2 e^{-y^2}\mathrm{d}y - x\int_{\sqrt{x}}^\infty e^{-y^2}\mathrm{d}y.$$

In [52], we have

$$\int_\mu^\infty x^m e^{-\beta x^n}\mathrm{d}x = \frac{\Gamma(\nu,\beta\mu^n)}{n\beta^\nu} \tag{3.10}$$

where $\nu = \frac{m+1}{n}$. Thus, we can rewrite I as

$$I = \frac{1}{2}\left(\Gamma\left(\frac{3}{2},x\right) - \Gamma\left(\frac{1}{2},x\right)\right)$$

and then

$$\mathbb{E}\left[\frac{|h_{kj}|^2}{||\mathbf{h}_j||}\right] = \frac{1}{(K-2)!}\left[\int_0^\infty x^{K-2}\Gamma\left(\frac{3}{2},x\right)\mathrm{d}x - \int_0^\infty x^{K-1}\Gamma\left(\frac{1}{2},x\right)\mathrm{d}x\right] \tag{3.11}$$

Note that

$$\frac{1}{K-1}\int_0^\infty \Gamma\left(\frac{3}{2},x\right)\mathrm{d}x^{K-1} = \frac{1}{K-1}\left(K-\frac{1}{2}\right)!,$$

and

$$\frac{1}{K}\int_0^\infty \Gamma\left(\frac{1}{2},x\right)\mathrm{d}x^{K} = \frac{1}{K}\left(K-\frac{1}{2}\right)!.$$

Substitute them into (3.11), the mean of $\frac{|h_{kj}|^2}{||\mathbf{h}_j||}$ is given by

$$\begin{aligned}\mathbb{E}\left[\frac{|h_{kj}|^2}{||\mathbf{h}_j||}\right] &= \frac{(K-\frac{1}{2})!}{(K-2)!}\left[\frac{1}{K-1}-\frac{1}{K}\right] \\ &= \frac{(K-\frac{1}{2})!}{K!}\end{aligned}$$

Next, we calculate the variance of $\frac{|h_{kj}|^2}{|\mathbf{h}_j|}$, expressed as

$$\mathrm{Var}\left[\frac{|h_{kj}|^2}{|\mathbf{h}_j|}\right] = \mathbb{E}\left[\frac{A_{kj}^2}{A_{kj}+B_{kj}}\right] - \left(\mathbb{E}\left[\frac{A_{kj}}{\sqrt{A_{kj}+B_{kj}}}\right]\right)^2$$

Notice that the second term has been solved before. Next, we calculate the first term .

$$\begin{aligned}\mathbb{E}\left[\frac{A_{kj}^2}{A_{kj}+B_{kj}}\right] &= \frac{1}{(K-2)!}\int_{0^+}^{\infty}\int_{0^+}^{\infty}\frac{x^2}{x+y}e^{-(x+y)}y^{K-2}\mathrm{d}x\mathrm{d}y \\ &= \frac{1}{(K-2)!}\int_{0^+}^{\infty}y^{K-2}\int_{y}^{\infty}\frac{(z-y)^2}{z}e^{-z}\mathrm{d}z\mathrm{d}y.\end{aligned}$$

Since

$$\int_y^{\infty}\frac{(z-y)^2}{z}e^{-z}\mathrm{d}z = \int_y^{\infty}ze^{-z}\mathrm{d}z - 2y\int_y^{\infty}e^{-z}\mathrm{d}z + y^2\int_y^{\infty}z^{-1}e^{-z}\mathrm{d}z,$$

using (3.10), we have

$$\mathbb{E}\left[\frac{A_{kj}^2}{A_{kj}+B_{kj}}\right] = \frac{2}{K+1}.$$

Thus the variance of $\frac{|h_{kj}|^2}{||\mathbf{h}_j||}$ is calculated as

$$\mathrm{Var}\left[\frac{|h_{kj}|^2}{||\mathbf{h}_j||}\right] = \frac{2}{K+1} - \left(\frac{(K-\frac{1}{2})!}{K!}\right)^2$$

With $\mathbb{E}\left[\frac{|h_{kj}|^2}{||\mathbf{h}_j||}\right]$ and $\mathrm{Var}\left[\frac{|h_{kj}|^2}{||\mathbf{h}_j||}\right]$, (3.9) can be obtained using central limit theory.

□

Based on Lemma 3.1, when $M \gg 1$, the distribution of X_k can be approximated as follows:

$$X_k \sim \mathcal{N}\left(\sqrt{K}\frac{(K-\frac{1}{2})!}{K!}, \frac{2K}{M(K+1)} - \frac{K}{M}\left(\frac{(K-\frac{1}{2})!}{K!}\right)^2\right).$$

By this approximation, the mean of X_k^2 can be calculated by

$$\begin{aligned}\mu_{X_k^2} &= \mathrm{Var}[X_k] + \mathbb{E}^2[X_k] \\ &= \frac{M-1}{M}\left(\frac{(K-\frac{1}{2})!}{K!}\right)^2 K + \frac{2K}{(K+1)M}\end{aligned}$$

The variance of X_k^2 can be expressed as

$$\mathrm{Var}[X_k^2] = \mathbb{E}[X_k^4] - \mathbb{E}^2[X_k^2].$$

To calculate the mean of X_k^4, we use the MGF of Gaussian distribution

$$M_x(t) = \exp\left(\mu t + \frac{1}{2}\sigma^2 t^2\right),$$

where μ and σ^2 are the mean and the variance. Then the expectation of X_k^4 are

$$\begin{aligned}\mathbb{E}[X_k^4] &= M_x^{(4)}(0) \\ &= 3\sigma^4 + 6\mu^2\sigma^2 + \mu^4.\end{aligned}$$

So the variance of X_k^4 is given by

$$\begin{aligned}\mathrm{Var}[X_k^4] &= 2\sigma^4 + 4\sigma^2\mu^2 \\ &= \left[\frac{8K^2}{K+1}\left(\frac{(K-\frac{1}{2})!}{K!}\right)^2 - 4K^2\left(\frac{(K-\frac{1}{2})!}{K!}\right)^4\right]\frac{1}{M} + o\left(\frac{1}{M}\right)\end{aligned}$$

We can see that the variance of the received signal power is very small for large M and converges to 0 as $M \to \infty$. By the law of large numbers, the signal power converges to its average as the number of antennas increases.

Next, we investigate the distribution of the interference power component Y_k defined in (3.7). The following proposition is obtained.

Proposition 2. *When $M \gg 1$, the pdf of Y_k has the following approximation:*

$$f_{Y_k}(y) = \frac{r}{\lambda\,(1-r)^{K-2}}\left[e^{-\frac{y}{\lambda}r} - e^{-\frac{y}{\lambda}}\sum_{n=0}^{K-3}\left(\frac{1-r}{\lambda}\right)^n \frac{y^n}{n!}\right], \tag{3.12}$$

where

$$\rho = \frac{1}{M}\frac{K^2+7K}{(K-1)(K-2)}, \tag{3.13}$$

$$\lambda = \frac{K}{K+1} - \sqrt{\rho}, \tag{3.14}$$

$$r = \frac{K-(K+1)\sqrt{\rho}}{K+(K+1)(K-2)\sqrt{\rho}}. \tag{3.15}$$

Proof. Recall that

$$Y_k \triangleq \sum_{i=1, i\neq k}^{K} \frac{1}{M}\left|\sum_{j=1}^{M}\frac{\sqrt{K}}{||\mathbf{h}_j||}h_{kj}\overline{h}_{ij}\right|^2.$$

In order to find the distribution of Y_k, we first investigate the distribution of $\frac{\sqrt{K}}{||\mathbf{h}_j||}h_{kj}\overline{h}_{ij}$. Denote $h_{nj} = x_{nj} + \mathrm{i}y_{nj}$ where x_{nj} and y_{nj} are the real and imaginary part of h_{nj} respectively, both following i.i.d. $\mathcal{N}(0, 1/2)$. Then $h_{kj}\overline{h}_{ij}$ and $||\mathbf{h}_j||$ can be written by

$$h_{kj}\overline{h}_{ij} = (x_{kj}x_{ij} + y_{kj}y_{ij}) - \mathrm{i}(x_{kj}y_{ij} + x_{ij}y_{kj}),$$
$$||\mathbf{h}_j|| = \sqrt{x_{kj}^2 + y_{kj}^2 + x_{ij}^2 + y_{ij}^2 + z},$$

where $z = \sum_{t=1, t\neq k, i}^{K} |h_{tj}|^2$ is distributed as $\mathrm{Erlang}(K-2, 1)$ and the pdf of z is $f_z(z) = \frac{z^{K-3}}{(K-3)!}e^{-z}$. Then the mean of $\frac{\sqrt{K}}{||\mathbf{h}_j||}h_{kj}\overline{h}_{ij}$ is given by

$$\mathbb{E}\left[\frac{\sqrt{K}}{||\mathbf{h}_j||}h_{kj}\overline{h}_{ij}\right] = \mathbb{E}\left[\frac{x_{kj}x_{ij} + y_{kj}y_{ij}}{\sqrt{x_{kj}^2+y_{kj}^2+x_{ij}^2+y_{ij}^2+z}}\right] + \mathrm{i}\mathbb{E}\left[\frac{x_{kj}y_{ij} + x_{ij}y_{kj}}{\sqrt{x_{kj}^2+y_{kj}^2+x_{ij}^2+y_{ij}^2+z}}\right].$$

Since the integral of an odd function over a symmetric interval is 0, the real part and the imaginary part both equal to 0. So we have

$$\mathbb{E}\left[\frac{\sqrt{K}}{||\mathbf{h}_j||}h_{kj}\overline{h}_{ij}\right] = 0.$$

Since the average of $\frac{\sqrt{K}}{||\mathbf{h}_j||}h_{kj}\overline{h}_{ij}$ is 0, the variance of $\frac{\sqrt{K}}{||\mathbf{h}_j||}h_{kj}\overline{h}_{ij}$ is given by

$$\mathrm{Var}\left[\frac{\sqrt{K}}{||\mathbf{h}_j||}h_{kj}\overline{h}_{ij}\right] = K \cdot \mathbb{E}\left[\frac{|h_{kj}|^2|h_{ij}|^2}{|h_{kj}|^2 + |h_{ij}|^2 + \sum_{t=1,t\neq k,i}^{K}|h_{tj}|^2}\right] \tag{3.16}$$

Recall that $|h_{nj}|^2$ follows an exponential distribution with the rate parameter of 1 and $\sum_{t=1,t\neq k,i}^{K}|h_{tj}|^2 \sim \mathrm{Erlang}(K-2,1)$. With integral calculations, the variance of $\frac{\sqrt{K}}{||\mathbf{h}_j||}h_{kj}\overline{h}_{ij}$ is given by

$$\mathrm{Var}\left[\frac{\sqrt{K}}{||\mathbf{h}_j||}h_{kj}\overline{h}_{ij}\right] = \frac{K}{K+1}.$$

By central limit theory, the distribution of

$$\frac{1}{\sqrt{M}}\sum_{j=1}^{M}\frac{\sqrt{K}}{||\mathbf{h}_j||}h_{kj}\overline{h}_{ij}$$

can be approximated as $\mathcal{CN}\left(0, K/(K+1)\right)$ for $M \gg 1$. Then the ith term of Y_k, which is

$$Y_{k,i} \triangleq \left|\frac{1}{\sqrt{M}}\sum_{j=1}^{M}\frac{\sqrt{K}}{||\mathbf{h}_j||}h_{kj}\overline{h}_{ij}\right|^2 \quad \text{for } i \neq k$$

is distributed as $\mathrm{Gamma}\left(1, K/(K+1)\right)$.

Next we calculate the correlation coefficient $\rho_{i,m}$ of $Y_{k,i}$ and $Y_{k,m}$ for $i \neq m$, defined as

$$\rho_{i,m} = \frac{\mathrm{Cov}(Y_{k,i}Y_{k,m})}{\sqrt{\mathrm{Var}[Y_{k,i}]\mathrm{Var}[Y_{k,m}]}}.$$

Since $Y_{k,i} \sim \text{Gamma}\,(1, K/(K+1))$, we have

$$\mathbb{E}[Y_{k,i}] = \frac{K}{K+1}, \quad \text{Var}[Y_{k,i}] = \frac{K^2}{(K+1)^2}.$$

The covariance of $\text{Cov}[Y_{k,i}Y_{k,m}]$ is

$$\begin{aligned}\text{Cov}[Y_{k,i}Y_{k,m}] &= \mathbb{E}[Y_{k,i}Y_{k,m}] - \mathbb{E}[Y_{k,i}]\mathbb{E}[Y_{k,m}] \\ &= \mathbb{E}[Y_{k,i}Y_{k,m}] - \frac{K^2}{(K+1)^2},\end{aligned}$$

where

$$\begin{aligned}&\mathbb{E}(Y_{k,i}Y_{k,m}) = \frac{K^2}{M^2}\mathbb{E}\left[\left|\sum_{j=1}^{M}\frac{h_{kj}\overline{h}_{ij}}{||\mathbf{h}_j||}\right|^2\left|\sum_{j=1}^{M}\frac{h_{kj}\overline{h}_{mj}}{||\mathbf{h}_j||}\right|^2\right] \\ &= \frac{K^2}{M^2}\mathbb{E}\left[\sum_{j=1}^{M}\frac{|h_{kj}|^4|h_{ij}|^2|h_{mj}|^2}{||\mathbf{h}_j||^4} + \sum_{j=1}^{M}\sum_{l=1,l\neq j}^{M}\frac{|h_{kj}|^2|h_{ij}|^2}{||\mathbf{h}_j||^2}\frac{|h_{kl}|^2|h_{ml}|^2}{||\mathbf{h}_l||^2}\right] \\ &= \frac{K^2}{M^2}\sum_{j=1}^{M}\mathbb{E}\left[\frac{|h_{kj}|^4|h_{ij}|^2|h_{mj}|^2}{||\mathbf{h}_j||^4}\right] + \frac{K^2}{M^2}\sum_{j=1}^{M}\sum_{l=1,l\neq j}^{M}\mathbb{E}\left[\frac{|h_{kj}|^2|h_{ij}|^2}{||\mathbf{h}_j||^2}\right]\mathbb{E}\left[\frac{|h_{kl}|^2|h_{ml}|^2}{||\mathbf{h}_l||^2}\right].\end{aligned}$$

From (3.16), we can calculate $\mathbb{E}\left[\frac{|h_{kj}|^2|h_{ij}|^2}{||\mathbf{h}_j||^2}\right]$ as

$$\mathbb{E}\left[\frac{|h_{kj}|^2|h_{ij}|^2}{||\mathbf{h}_j||^2}\right] = \frac{1}{K+1},$$

and

$$\mathbb{E}(Y_{k,i}Y_{k,m}) = \frac{K^2}{M^2}\sum_{j=1}^{M}\mathbb{E}\left[\frac{|h_{kj}|^4|h_{ij}|^2|h_{mj}|^2}{||\mathbf{h}_j||^4}\right] + \frac{M-1}{M}\frac{K^2}{(K+1)^2}.$$

Notice that h_{nj} $(n = 1, \cdots, K)$ is one of the entries in the vector $\mathbf{h}_j$. Thus $|h_{nj}|^2$ and $||\mathbf{h}_j||^4$ are correlated. But for large or moderate K, e.g., a few tens, their dependence is small. For tractable analysis, we treat $||\mathbf{h}_j||^4$ as an independent random

variable to $|h_{nj}|^2$. So the average of $\frac{|h_{kj}|^4|h_{ij}|^2|h_{mj}|^2}{||\mathbf{h}_j||^4}$ is approximated as

$$\mathbb{E}\left[\frac{|h_{kj}|^4|h_{ij}|^2|h_{mj}|^2}{||\mathbf{h}_j||^4}\right] \approx \mathbb{E}\left[|h_{kj}|^4\right] \cdot \mathbb{E}\left[|h_{ij}|^2\right] \cdot \mathbb{E}\left[|h_{mj}|^2\right] \cdot \mathbb{E}\left[\frac{1}{||\mathbf{h}_j||^4}\right]$$

Recall that $|h_{kj}|^2$ has exponential distribution with rate parameter of 1, then we have

$$\mathbb{E}\left[|h_{kj}|^4\right] = 2, \quad \mathbb{E}\left[|h_{ij}|^2\right] = \mathbb{E}\left[|h_{mj}|^2\right] = 1.$$

Since $||\mathbf{h}_j||^2$ is the sum of K exponential random variable $\{h_{kj}\}_{k=1}^K$, it follows the distribution of $\mathrm{Earlang}(K, 1)$. Then the average of $\frac{1}{||\mathbf{h}_j||^4}$ is calculated as

$$\begin{aligned}\mathbb{E}\left[\frac{1}{||\mathbf{h}_j||^4}\right] &= \int_0^\infty \frac{x^{K-3}e^{-x}}{(K-1)!}\mathrm{d}x \\ &= \frac{1}{(K-1)(K-2)}.\end{aligned}$$

Then we have

$$\mathbb{E}(Y_{k,i}Y_{k,m}) = \frac{2K^2}{M(K-1)(K-2)} + \frac{M-1}{M}\frac{K^2}{(K+1)^2}.$$

So the correlation coefficient can be calculated as

$$\begin{aligned}\rho_{i,m} &= \frac{(K+1)^2}{K^2}\left(\mathbb{E}(Y_{k,i}Y_{k,m}) - \frac{K^2}{(K+1)^2}\right) \\ &= \frac{K^2+7K}{M(K-1)(K-2)}.\end{aligned}$$

It can be observed that $Y_k = \sum_{i\neq k}^K Y_{k,i}$ is the sum of $K-1$ correlated gamma variables, and the correlation coefficient of any two variables is

$$\rho = \frac{K^2+7K}{M(K-1)(K-2)}.$$

From Corollary 1 of [45], the pdf of Y_k is given by

$$f_{Y_k}(y) = \prod_{n=1}^{K-1} \frac{\sigma_1}{\sigma_n} \sum_{t=0}^{\infty} \frac{\delta_t y^{K+t-2} e^{-y/\sigma_1}}{\sigma_1^{K+t-1}\Gamma(K+t-1)}, \tag{3.17}$$

where $\sigma_1 \leq \sigma_2 \leq \cdots \leq \sigma_{K-1}$ are the ordered eigenvalues of the $(K-1) \times (K-1)$ matrix $\mathbf{G}$ whose diagonal entries are $K/(K+1)$ and off-diagonal entries are $\sqrt{\rho}K/(K+1)$, and δ_t's are defined iteratively as

$$\begin{aligned} &\delta_0 = 1, \\ &\delta_{t+1} = \frac{1}{t+1} \sum_{m=1}^{t+1} \left[\sum_{n=1}^{K-1} \left(1 - \frac{\sigma_1}{\sigma_n}\right)^m \right] \delta_{t+1-m}. \end{aligned} \tag{3.18}$$

The eigenvalues of $\mathbf{G}$ can be calculated to be

$$\begin{aligned} \sigma_1 = \cdots = \sigma_{K-2} &= \frac{K}{K+1} - \sqrt{\rho} \\ \sigma_{K-1} &= \frac{K}{K+1} + (K-2)\sqrt{\rho}. \end{aligned} \tag{3.19}$$

Using (3.18)-(3.19), we have

$$\delta_t = \left(1 - \frac{\sigma_1}{\sigma_{K-1}}\right)^t. \tag{3.20}$$

Then the pdf of Y_k can be rewritten by the Taylor Series expansion of exponential functions as

$$\begin{aligned} f_{Y_k}(y) &= \frac{\sigma_1}{\sigma_{K-1}} \sum_{n=K-2}^{\infty} \frac{(1 - \frac{\sigma_1}{\sigma_{K-1}})^{n-K+2} y^n e^{-y/\sigma_1}}{\sigma_1^{n+1}\Gamma(n+1)} \\ &= \frac{1}{\sigma_{K-1}} \left(1 - \frac{\sigma_1}{\sigma_{K-1}}\right)^{-(K-2)} \left[e^{-y/\sigma_{K-1}} - e^{-y/\sigma_1} \sum_{n=0}^{K-3} \left(\frac{1}{\sigma_1} - \frac{1}{\sigma_{K-1}}\right)^n \frac{y^n}{n!} \right] \end{aligned}$$

By denoting $r = \sigma_1/\sigma_{K-1}$, we obtain (3.12). □

The mean and the variance of Y_k can be calculated by using the results derived

in Equation (2.16) and Equation (2.19). We have

$$\mu_{Y_k} = \mathbb{E}[Y_k] = (K-2)\sigma_1 + \sigma_{K-1} = \frac{K(K-1)}{K+1},$$
$$\mathrm{Var}[Y_k] = (K-2)\sigma_1^2 + \sigma_{K-1}^2 = (K-1)\left(\frac{K}{K+1}\right)^2 + \frac{K(K+7)}{M}.,$$

We can see that for any fixed K, the variance of Y_k does not diminish to 0 as M increases. Thus it cannot be seen as deterministic even for large M.

3.4 Performance Analysis

Similar with Chapter 2, since the variations of the signal power component X_k^2 is relatively small to the variations of the interference power Y_k, we treat the signal power random variable as a constant and keep the interference power Y_k as random. Then, we derive the analytical results of the outage probability and the system sum-rate by using the pdf of the interference power.

3.4.1 Outage Probability Analysis

Recall that γ_{th} is the SINR threshold. By replacing X_k^2 with its mean value $\mu_{X_k^2}$, the outage probability can be approximated as follows

$$P_{\text{out}} \approx \mathbb{P}\left(\frac{P_t M}{K}\frac{\mu_{X_k^2}}{1+\frac{P_t}{K}Y_k} < \gamma_{th}\right)$$
$$= \begin{cases} 1 & \text{if } \gamma_{th} \geq \frac{P_t M}{K}\mu_{X_k^2} \\ \mathbb{P}\left(Y_k > \frac{M}{\gamma_{th}}\mu_{X_k^2} - \frac{K}{P_t}\right) & \text{otherwise} \end{cases}.$$

When $\gamma_{th} < \frac{P_t M}{K}\mu_{X_k^2}$, based on (3.12), we can calculate the outage probability of the modified MRT as

$$P_{\text{out}} \approx (1-r)^{-(K-2)}\, e^{-\frac{r}{\lambda}\left(\frac{M}{\gamma_{th}}\mu_{X_k^2} - \frac{K}{P_t}\right)} - (1-r)^{-(K-2)}$$
$$\times \sum_{n=0}^{K-3} \frac{r}{n!}(1-r)^n \Gamma\left(n+1, \frac{1}{\lambda}\left(\frac{M}{\gamma_{th}}\mu_{X_k^2} - \frac{K}{P_t}\right)\right). \tag{3.21}$$

The parameters are defined in (3.13)-(3.15).

The analytical outage probability with MRT precoding in (2.20) can also be represented by formula (3.21) but with different parameter values:

$$\rho_{\mathrm{MRT}} = \frac{1}{M}, \quad r_{\mathrm{MRT}} = \frac{1-\sqrt{\rho_{\mathrm{MRT}}}}{1+(K-2)\sqrt{\rho_{\mathrm{MRT}}}},$$
$$\lambda_{\mathrm{MRT}} = 1-\sqrt{\rho_{\mathrm{MRT}}}, \quad \mu_{X_k^2,\mathrm{MRT}} \approx 1.$$

When $K, M \to \infty$ but with a fixed ratio of M/K, the parameters of the modified MRT precoding converge to the parameters of the MRT precoding. Then the outage probability formulas of the two schemes are the same. This can be explained from the modified MRT precoding formula in (3.3). As $K \to \infty$, the random variable $|\mathbf{h}_j|^2/K$ converges to 1 using the law of large numbers. Thus the diagonal matrix $\mathbf{D}$ converges to an identity matrix and the modified MRT precoding converges to the MRT precoding. When K is finite and small compared to M, the outage probabilities of the two precodings are different. In practice, massive MIMO systems have finite M (usually no more than a few hundreds) due to the hardware and computation limitations. Also the number of served users K is usually moderate (no more than a few tens) due to the desired quality-of-service. Under such practice scenario, simulation in Section 3.5 shows that modified MRT precoding has lower outage probability.

3.4.2 Sum-Rate Analysis

In Section 3.4, we approximate the SINR at User k as

$$\mathrm{SINR}_k = \frac{P_t M}{K} \frac{\mu_{X_k^2}}{1+\frac{P_t}{K}Y_k}.$$

Using this approximation, the average achievable rate at User k can be written as

$$\mathbb{E}[\mathrm{R}_k] = \mathbb{E}\left[\log_2\left(1+\frac{P_t M}{K}\frac{\mu_{X_k^2}}{1+\frac{P_t}{K}Y_k}\right)\right]$$

$$= \log_2\left(1+\frac{P_t}{K}M\mu_{X_k^2}\right) + \mathbb{E}\left[\log_2\left(1+\frac{P_t}{K+P_tM\mu_{X_k^2}}Y_k\right)\right] - \mathbb{E}\left[\log_2\left(1+\frac{P_t}{K}Y_k\right)\right].$$

With the pdf of Y_k in (3.12) and the integral formula in (2.22), the average sum-rate with modified MRT precoding is given by

$$\begin{aligned}\mathbb{E}[R_{\text{sum}}] = K\cdot\Bigg\{&\log_2\left(1+\frac{P_t}{K}M\mu_{X_k^2}\right)+\frac{(1-r)^{-(K-2)}}{\ln 2}e^{\frac{Kr}{\lambda P_t}}\Bigg[\exp\left(\frac{rM\mu_{X_k^2}}{\lambda}\right)\\ &\cdot E_1\left(\frac{r(K+P_tM\mu_{X_k^2})}{\lambda P_t}\right)-E_1\left(\frac{Kr}{\lambda P_t}\right)\Bigg]-\frac{r(1-r)^{-(K-2)}}{\ln 2}e^{\frac{K}{\lambda P_t}}\\ &\cdot\Bigg[e^{\frac{M\mu_{X_k^2}}{\lambda}}\sum_{n=0}^{K-3}(1-r)^n\sum_{i=0}^{n}E_{i+1}\left(\frac{K+P_tM\mu_{X_k^2}}{\lambda P_t}\right)-\sum_{n=0}^{K-3}(1-r^n)\\ &\cdot\sum_{n=0}^{K-3}(1-r)^n\sum_{i=0}^{n}E_{i+1}\left(\frac{K}{\lambda P_t}\right)\Bigg]\Bigg\}\end{aligned} \tag{3.22}$$

and the outage capacity can be written as

$$R_{\text{out}} = (1-P_{\text{out}})\cdot R_{\text{sum}}. \tag{3.23}$$

3.5 Simulation Results

In this section, we verify our analytical results and compare the performance of the MRT precoding with the performance of the modified MRT precoding.

In Fig. 3.1, the pdf of the interference power is drawn. The number of antennas is 100, and the number of users is assumed to be 10 and 30. Since (3.12) is the closed-form of the infinite summation series, the large tail terms are remained and (3.12) has a tight match to the Monte-Carlo simulation.

Fig. 3.2 shows the outage probability for different number of users ranging from 10 to 30. The number of antennas at the BS is 100. The total transmit power and the SINR threshold are 10dB and 7dB respectively. It can be observed that the outage probability increases rapidly as the number of users increases. In the proof of Proposition 2, we treat the random variables $|h_{nj}|^2$ and $|\mathbf{h}_j|^4$ as independent to

simplify the derivation. However, the assumption relies on a large K. So the gap between the analytical result and the Monte-Carlo simulation is noticeable when K is 10. However, as K increases to 12, our result still tightly match to the simulation. From the figure, it can be seen that the modified MRT precoding performs better than the MRT precoding for all range of K.

In Fig. 3.3, the outage probability with different total transmit power is given. The SINR threshold is 7dB. The number of users and the number of antennas are 15 and 100 respectively. The figure shows that the outage probability does not decrease to 0 as the total transmit power increases. Similar with MRT precoding, the modified precoding is interference limited. It is also shown that the modified MRT precoding has a lower outage probability than MRT precoding.

Fig. 3.4 shows the system sum-rate for different number of users ranging from 2 to 20. The total transmit power is assumed as 10dB. As K increases, the sum-rate with the modified precoding has a nearly linear growth. Also, it is also shown that the sum-rate of the modified MRT precoding is greater than the sum-rate of MRT precoding for all range of K.

Fig. 3.5 shows the sum-rate for different number of antennas ranging from 50 to 290. The total transmit power is 10dB. As the number of antennas M increases, the system sum-rate with modified MRT precoding increases and is higher than the sum-rate of MRT precoding for all range of M.

Fig. 3.6 shows the outage capacity for different number of users ranging from 5 to 30. The number of antennas is assumed as 100. The total transmit power P_t is 10dB and the SINR threshold is 5dB. It is shown that the outage capacity still increases as K increases from 5 to 20. When K is larger than 20, the outage capacity starts decreasing due to high outage probability. The outage capcity of the modified MRT precoding is greater than the outage capacity of MRT precoding, because the modified MRT precoding performs better than MRT precoding both for the outage probability and the sum-rate.

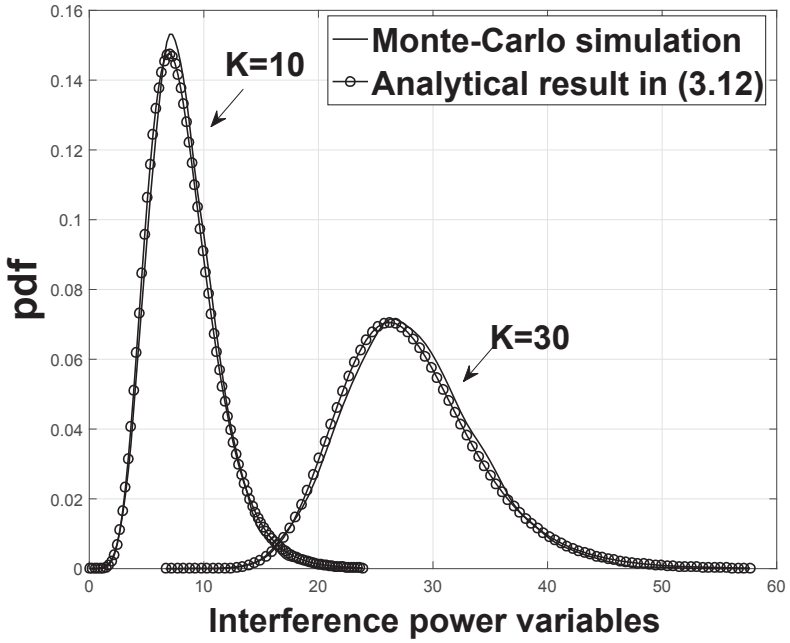

Fig. 3.1. The pdf of the interference power. $M = 100$.

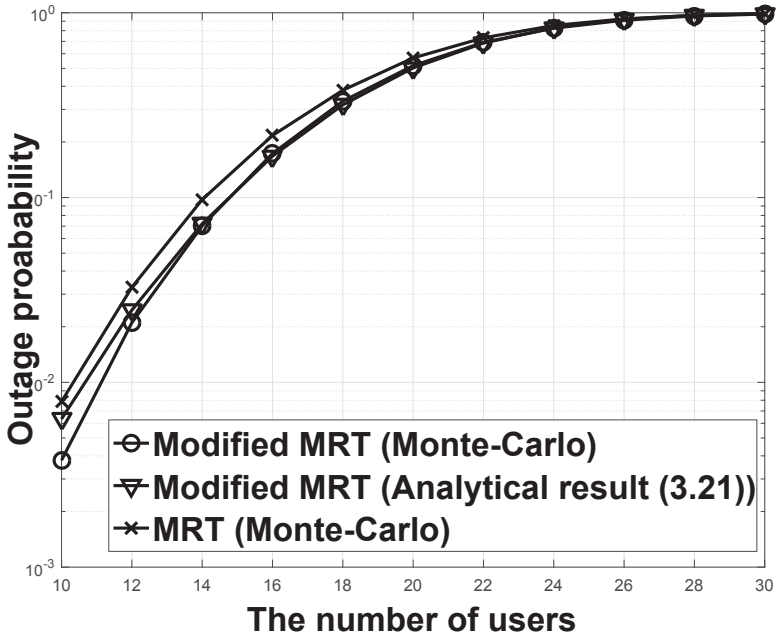

Fig. 3.2. Outage probability v.s. K. $M = 100$, $P_t = 10$dB, $\gamma = 7$dB.

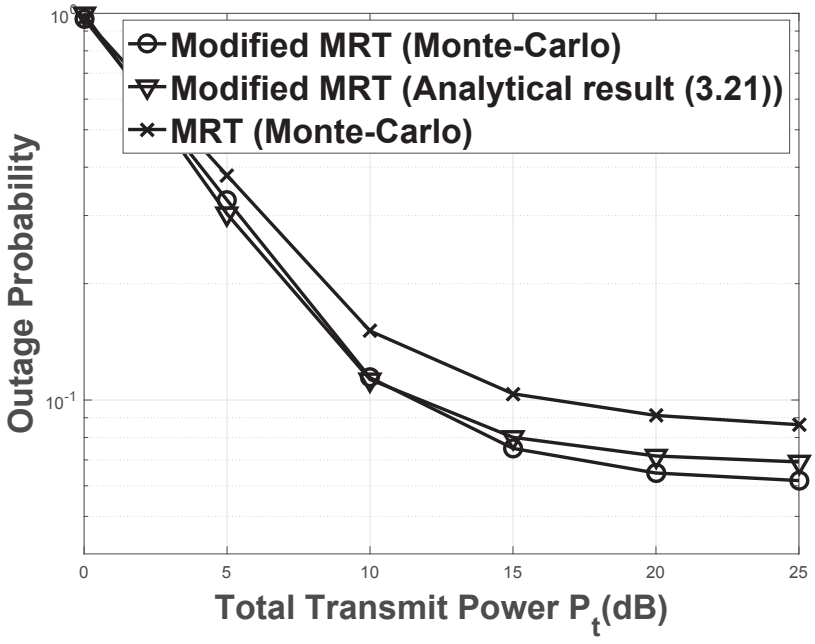

Fig. 3.3. Outage probability v.s. P_t. $M = 100$, $K = 15$, $\gamma = 7$dB.

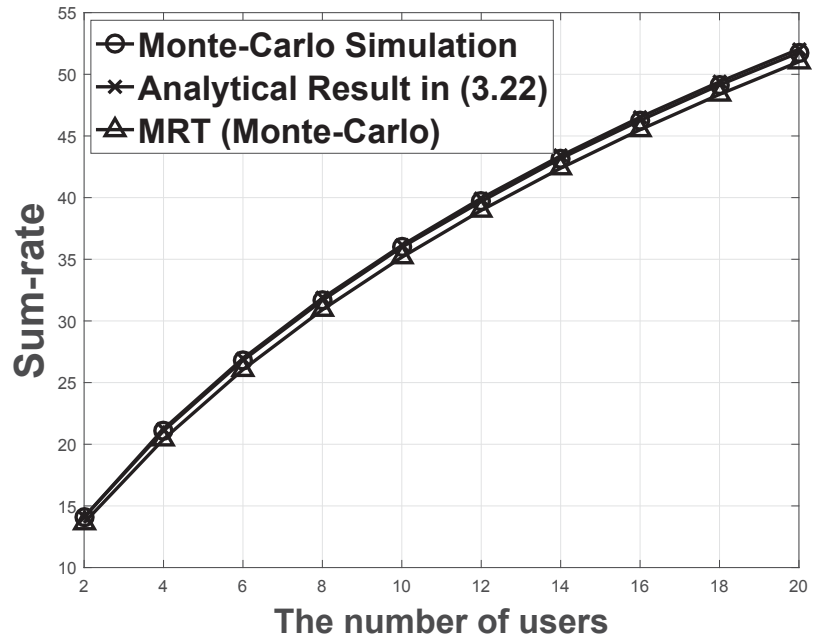

Fig. 3.4. Sum-rate v.s. K. $M = 100$, $P_t = 10$dB.

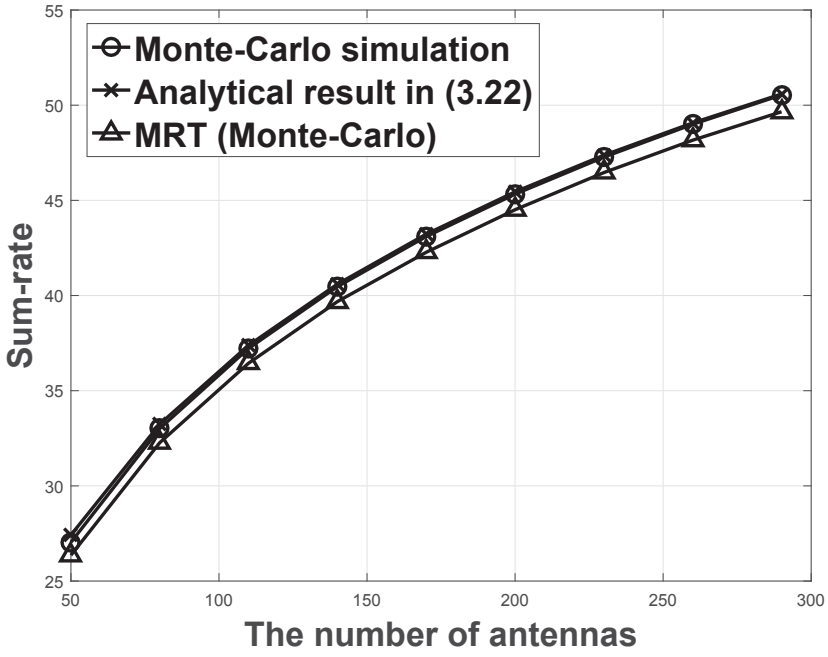

Fig. 3.5. Sum-rate v.s. M. $K = 10$, $P_t = 10$dB.

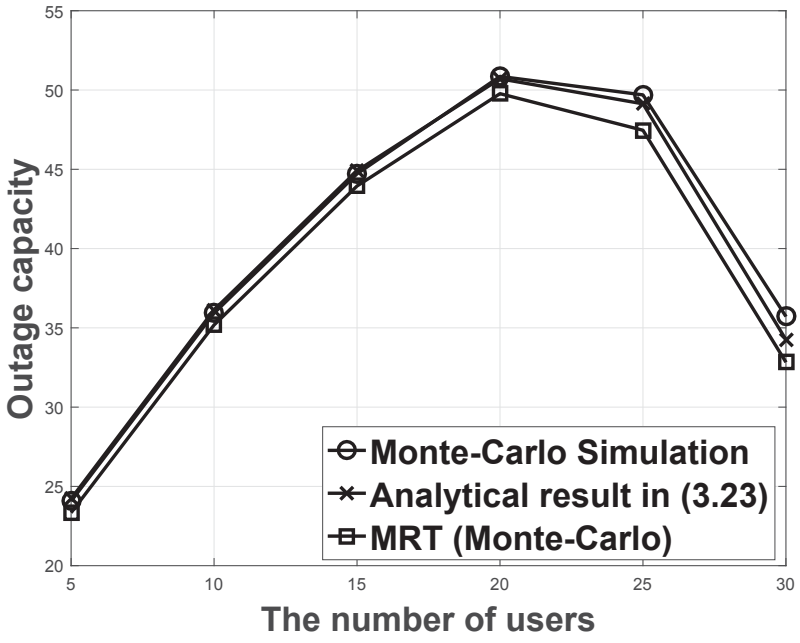

Fig. 3.6. Outage capacity vs. K. $M = 100$, $P_t = 10$dB, $\gamma_{th} = 5$dB.

3.6 Conclusion

In this chapter, we propose a modified MRT precoding under per-antenna transmit power constraint, while MRT precoding only considers the total transmit power constraint. By investigating the random properties of the received signal power and interference power, an approximate pdf of the interference power is derived. In addition, the analytical results of the outage probability and the sum-rate are derived for the large but finite number of antennas and the moderate number of users. Also, we compare our results with MRT precoding. The simulation results show that the modified MRT precoding performs better than MRT precoding on both the outage probability and the sum-rate.

Chapter 4

Conclusion and Future Work

Massive MIMO is one of the most promising technologies for next generation cellular systems. Compared to conventional MIMO, due to the excess spatial resources, massive MIMO can provide significantly higher throughput, link reliability, energy efficiency. There are a lot of existing work on the sum-rate performance analysis of massive MIMO. However, there are very little investigations on the outage probability. Since the outage probability analysis requires the knowledge of the random properties of the SINR, the asymptotically deterministic SINR results and the method in existing work are not applicable for the outage probability analysis. In our work, we preserve the random nature of the interference power and investigate its distribution. This new approach allows the outage probability calculation. Moreover, the practical per-antenna power constraint is considered for the multi-user massive MIMO system. To accommodate the per-antenna power constraint, we design a modified MRT precoding and derive its performance.

Chapter 2 is on the multi-user massive MIMO with MRT precoding. Assuming a single-cell network with perfect CSI, the pdf of the interference power term in SINR is derived with the help of central limit theory. Based on the pdf result, the analytical results of the outage probability and the sum-rate are calculated by integrals. The simulation results show that the sum-rate increases with the increasing number of users, while the outage probability decreases on the contrary.

Chapter 3 extends the research to the per-antenna power constraint scenario

which is more practical for the BS in cellular systems. A modified MRT precoding is proposed under per-antenna transmit power constraint. By following the methods of the first work, the pdf of the interference power are derived. Then the outage probability and the sum-rate of the new precoding scheme are investigated. The simulation results show that the modified MRT precoding can achieve lower outage probability even with the more strict power constraint.

In the future work, more practical system models can be considered. Some possible extensions are discussed in what follows.

- Channel errors

  In real scenarios, channel errors exist when the BS estimates the CSI by uplink training. Then the BS will have imperfect CSI instead of perfect CSI. It is important to analyze the performance of the precoding schemes for massive MIMO with imperfect CSI to understand the effect of CSI error.

- Correlated channels

  With the large number of BS antennas in massive MIMO, antenna spacing is limited when the BS is designed with a moderate size and then channel correlation is inevitable. The performance analysis of massive MIMO systems with correlated channels can be helpful in deciding the antenna spacing in antenna arrays and the size of BSs.

- Pilot contamination

  As mentioned in Section 1.6, when the number of transmit antennas goes to infinity, the channels from the BS to the individual users becomes close-to-orthogonal from each other. Thus the effects of small-fading and user-interference diminish. On the contrary, pilot contamination caused by pilot sharing becomes a more prominent challenge in massive MIMO systems. One future direction is to extend our work to multi-cell massive MIMO system with pilot contribution.

- Millimeter wave (mmWave)

The use of mmWave is another potential direction for the next generation cellular systems. Millimeter wave refers to extremely high frequency signals ranging from 30GHz to 300 GHz (gigahertz). Due to the huge bandwidth of mmWave, high data rate transmission can be provided. However, there are a few challenges such as high propagation loss and sensitivity to blockage. Performance analysis of massive MIMO using mmWave is a fast growing research topic.

References

[1] J. C. Maxwell, "A dynamical theory of the electromagnetic field." *Proceedings of the Royal Society of London*, vol. 13, pp. 531–536, 1863.

[2] T. S. Rappaport, "Wireless communications–principles and practice, (the book end)," *Microwave Journal*, vol. 45, no. 12, pp. 128–129, 2002.

[3] D. Tse and P. Viswanath, *Fundamentals of wireless communication*. Cambridge university press, 2005.

[4] A. F. Molisch, *Wireless communications*. John Wiley & Sons, 2007.

[5] M. Mouly, M.-B. Pautet, and T. Foreword By-Haug, *The GSM system for mobile communications*. Telecom publishing, 1992.

[6] S. Redl, M. W. Oliphant, M. K. Weber, and M. K. Weber, *An introduction to GSM*. Artech House, Inc., 1995.

[7] B. A. Series, "Mobile network evolution: a revolution on the move," *IEEE Communications magazine*, p. 104, 2002.

[8] S. J. Vaughan-Nichols, "Achieving wireless broadband with wimax," *Computer*, no. 6, pp. 10–13, 2004.

[9] S. M. Cherry, "Wimax and wi-fi: separate and unequal," *IEEE spectrum*, vol. 41, no. 3, pp. 16–16, 2004.

[10] S. Sesia, I. Toufik, and M. Baker, *LTE: the UMTS long term evolution*. Wiley Online Library, 2009.

[11] N. Alliance, "5g white paper," *Next Generation Mobile Networks, White paper*, 2015.

[12] F. Rusek, D. Persson, B. K. Lau, E. G. Larsson, T. L. Marzetta, O. Edfors, and F. Tufvesson, "Scaling up mimo: Opportunities and challenges with very large arrays," *Signal Processing Magazine, IEEE*, vol. 30, no. 1, pp. 40–60, 2013.

[13] E. Larsson, O. Edfors, F. Tufvesson, and T. Marzetta, "Massive mimo for next generation wireless systems," *Communications Magazine, IEEE*, vol. 52, no. 2, pp. 186–195, 2014.

[14] T. S. Rappaport, S. Sun, R. Mayzus, H. Zhao, Y. Azar, K. Wang, G. N. Wong, J. K. Schulz, M. Samimi, and F. Gutierrez, "Millimeter wave mobile communications for 5g cellular: It will work!" *IEEE access*, vol. 1, pp. 335–349, 2013.

[15] Z. Pi and F. Khan, "An introduction to millimeter-wave mobile broadband systems," *IEEE Communications Magazine*, vol. 49, no. 6, pp. 101–107, 2011.

[16] M. Elkashlan, T. Q. Duong, and H.-H. Chen, "Millimeter-wave communications for 5g: fundamentals: Part i [guest editorial]," *IEEE Communications Magazine*, vol. 52, no. 9, pp. 52–54, 2014.

[17] F. Boccardi, R. W. Heath, A. Lozano, T. L. Marzetta, and P. Popovski, "Five disruptive technology directions for 5g," *IEEE Communications Magazine*, vol. 52, no. 2, pp. 74–80, 2014.

[18] E. Biglieri, R. Calderbank, A. Constantinides, A. Goldsmith, A. Paulraj, and H. V. Poor, *MIMO wireless communications*. Cambridge university press, 2007.

[19] G. L. Stuber, J. R. Barry, S. W. Mclaughlin, Y. Li, M. A. Ingram, and T. G. Pratt, "Broadband mimo-ofdm wireless communications," *Proceedings of the IEEE*, vol. 92, no. 2, pp. 271–294, 2004.

[20] E. Telatar, "Capacity of multi-antenna gaussian channels," *European transactions on telecommunications*, vol. 10, no. 6, pp. 585–595, 1999.

[21] A. J. Paulraj, D. A. Gore, R. U. Nabar, and H. Bölcskei, "An overview of mimo communications-a key to gigabit wireless," *Proceedings of the IEEE*, vol. 92, no. 2, pp. 198–218, 2004.

[22] G. J. Foschini, "Layered space-time architecture for wireless communication in a fading environment when using multi-element antennas," *Bell labs technical journal*, vol. 1, no. 2, pp. 41–59, 1996.

[23] D. Gesbert, M. Kountouris, R. W. Heath Jr, C.-B. Chae, and T. Salzer, "Shifting the mimo paradigm," *IEEE signal processing magazine*, vol. 24, no. 5, pp. 36–46, 2007.

[24] G. Caire and S. Shamai, "On the achievable throughput of a multiantenna gaussian broadcast channel," *IEEE Transactions on Information Theory*, vol. 49, no. 7, pp. 1691–1706, 2003.

[25] S. Vishwanath, N. Jindal, and A. Goldsmith, "Duality, achievable rates, and sum-rate capacity of gaussian mimo broadcast channels," *IEEE Transactions on Information Theory*, vol. 49, no. 10, pp. 2658–2668, 2003.

[26] M. Joham, W. Utschick, and J. A. Nossek, "Linear transmit processing in mimo communications systems," *Signal Processing, IEEE Transactions on*, vol. 53, no. 8, pp. 2700–2712, 2005.

[27] T. M. Cover and J. A. Thomas, *Elements of information theory*. John Wiley & Sons, 2012.

[28] R. Esmailzadeh and M. Nakagawa, "Pre-rake diversity combination for direct sequence spread spectrum mobile communications systems," *IEICE Transactions on Communications*, vol. 76, no. 8, pp. 1008–1015, 1993.

[29] A. Wiesel, Y. C. Eldar, and S. Shamai, "Zero-forcing precoding and generalized inverses," *IEEE Transactions on Signal Processing*, vol. 56, no. 9, pp. 4409–4418, 2008.

[30] G. H. Golub and C. F. Van Loan, *Matrix computations*. JHU Press, 2012, vol. 3.

[31] C. B. Peel, B. M. Hochwald, and A. L. Swindlehurst, "A vector-perturbation technique for near-capacity multiantenna multiuser communication-part i: channel inversion and regularization," *IEEE Transactions on Communications*, vol. 53, no. 1, pp. 195–202, 2005.

[32] K.-H. Lee and D. Petersen, "Optimal linear coding for vector channels," *IEEE Transactions on Communications*, vol. 24, no. 12, pp. 1283–1290, 1976.

[33] M. Joham, K. Kusume, M. H. Gzara, W. Utschick, and J. A. Nossek, "Transmit wiener filter for the downlink of tddds-cdma systems," in *Spread Spectrum Techniques and Applications, 2002 IEEE Seventh International Symposium on*, vol. 1. IEEE, 2002, pp. 9–13.

[34] R. Choi and R. D. Murch, "Transmit mmse pre-rake pre-processing with simplified receivers for the downlink of miso tdd-cdma systems," in *Global Telecommunications Conference, 2002. GLOBECOM'02. IEEE*, vol. 1. IEEE, 2002, pp. 429–433.

[35] E. Bj, E. G. Larsson, T. L. Marzetta *et al.*, "Massive mimo: Ten myths and one critical question," *IEEE Communications Magazine*, vol. 54, no. 2, pp. 114–123, 2016.

[36] S. Yang and L. Hanzo, "Fifty years of mimo detection: The road to large-scale mimos," *IEEE Communications Surveys & Tutorials*, vol. 17, no. 4, pp. 1941–1988, 2015.

[37] T. L. Marzetta, "Noncooperative cellular wireless with unlimited numbers of base station antennas," *Wireless Communications, IEEE Transactions on*, vol. 9, no. 11, pp. 3590–3600, 2010.

[38] B. Gopalakrishnan and N. Jindal, "An analysis of pilot contamination on multi-user mimo cellular systems with many antennas," in *Signal Processing Advances in Wireless Communications (SPAWC), 2011 IEEE 12th International Workshop on*. IEEE, 2011, pp. 381–385.

[39] J. Jose, A. Ashikhmin, T. L. Marzetta, and S. Vishwanath, "Pilot contamination and precoding in multi-cell tdd systems," *Wireless Communications, IEEE Transactions on*, vol. 10, no. 8, pp. 2640–2651, 2011.

[40] J. Hoydis, S. Ten Brink, and M. Debbah, "Massive mimo in the ul/dl of cellular networks: How many antennas do we need?" *Selected Areas in Communications, IEEE Journal on*, vol. 31, no. 2, pp. 160–171, 2013.

[41] S. Wagner, R. Couillet, M. Debbah, and D. Slock, "Large system analysis of linear precoding in correlated miso broadcast channels under limited feedback," *Information Theory, IEEE Transactions on*, vol. 58, no. 7, pp. 4509–4537, 2012.

[42] H. Yang and T. L. Marzetta, "Performance of conjugate and zero-forcing beamforming in large-scale antenna systems," *Selected Areas in Communications, IEEE Journal on*, vol. 31, no. 2, pp. 172–179, 2013.

[43] X. Gao, O. Edfors, F. Rusek, and F. Tufvesson, "Linear pre-coding performance in measured very-large mimo channels," in *Vehicular Technology Conference (VTC Fall), 2011 IEEE*. IEEE, 2011, pp. 1–5.

[44] B. M. Hochwald, T. L. Marzetta, and V. Tarokh, "Multiple-antenna channel hardening and its implications for rate feedback and scheduling," *Information Theory, IEEE Transactions on*, vol. 50, no. 9, pp. 1893–1909, 2004.

[45] M.-S. Alouini, A. Abdi, and M. Kaveh, "Sum of gamma variates and performance of wireless communication systems over nakagami-fading channels," *Vehicular Technology, IEEE Transactions on*, vol. 50, no. 6, pp. 1471–1480, 2001.

[46] J. Wang, S. Jin, X. Gao, K.-K. Wong, and E. Au, "Statistical eigenmode-based sdma for two-user downlink," *Signal Processing, IEEE Transactions on*, vol. 60, no. 10, pp. 5371–5383, 2012.

[47] W. Yu and T. Lan, "Transmitter optimization for the multi-antenna downlink with per-antenna power constraints," *Signal Processing, IEEE Transactions on*, vol. 55, no. 6, pp. 2646–2660, 2007.

[48] K. Karakayali, R. Yates, G. Foschini, and R. Valenzuela, "Optimum zero-forcing beamforming with per-antenna power constraints," in *Information Theory, 2007. ISIT 2007. IEEE International Symposium on*. IEEE, 2007, pp. 101–105.

[49] S. K. Mohammed and E. G. Larsson, "Constant-envelope multi-user precoding for frequency-selective massive mimo systems," *Wireless Communications Letters, IEEE*, vol. 2, no. 5, pp. 547–550, 2013.

[50] M. Joham, W. Utschick, and J. Nossek, "On the equivalence of prerake and transmit matched filter," *Proc. ASST2001*, p. 3, 2001.

[51] J. Zhang and J. G. Andrews, "Adaptive spatial intercell interference cancellation in multicell wireless networks," *Selected Areas in Communications, IEEE Journal on*, vol. 28, no. 9, pp. 1455–1468, 2010.

[52] I. S. Gradshteyn and I. M. Ryzhik, *Table of integrals, series, and products*. Academic press, 2014.